

**Temporomandibular Joint Condylar/Fossa Positional Changes Post Herbst And Xbow  
Treatments In Adolescents Assessed Through CBCT Imaging**

by

Tareq Aldajani

A thesis submitted in partial fulfillment of the requirements for the degree of  
Master of Science

Medical Sciences – Oral Medicine

University of Alberta

© Tareq Aldajani, 2022

## **Abstract**

**Objective:** To evaluate the three-dimensional positional changes (anteroposterior, vertical, and mediolateral) in the condyle /and the glenoid fossa utilizing different Class II fixed mandibular positioners/appliances (Herbst and Xbow) compared to controls.

**Methods:** The primary sample consisted of 59 patients with Class II malocclusion between ten and sixteen years of age (10-14 females and 11-16 males). Patients were randomly allocated to one of the three groups (Herbst, Xbow, and control). Two CBCT images were taken for each patient, corresponding to pre-and post-treatment. The mandibular condyle and glenoid fossa position relative to the reference planes were assessed using Avizo© software using landmark to plane distance calculation. Reliability was assessed using ICC. MANOVA was conducted to determine whether the groups had a mean difference.

**Results:** Five patients were subsequently excluded because the time interval between T0 and T1 CBCT images was more than 16 months, resulting in a final sample size of 54 subjects (the average interval was 12.4 months). Regarding all dimensional positional changes (anteroposterior, mediolateral, and vertical), there was no significant difference in means of variations in the orthogonal distance of the condyle /and glenoid fossa landmarks based on groups ( $p > 0.05$ ).

**Conclusion:** All three groups had no significant differences ( $p > 0.05$ ) in the mean positional change in the condyle and fossa jointly, condyle separately, and fossa separately across all dimensions (anteroposterior, vertical and mediolateral) following treatment. Additionally, fixed

class II appliances (Herbst and Xbow) did not result in an additional or restrictive significant positional change in condyle relative to the fossa position compared to controls.

## PREFACE

This thesis is an original work by Tareq Aldajani. The CBCTs and data were gathered from patients who participated in a comprehensive project, “Skeletal, Functional And Dental Changes During Treatment Of Mild to Moderate Class II Malocclusions With Fixed Class II Correctors: A Randomized Clinical Trial” (Study ID of ethical approval Pro00045191). The University of Alberta's Health Research Ethics Board re-approved the project on January 21, 2022.

## ACKNOWLEDGEMENTS

I would like to thank Professor Manuel Lagravere and Dr. Reid Friesen's patience, guidance, and oversight. Their ethics, expertise, abilities, and compassion encouraged me. They never grumbled about addressing my many queries, nor did they lose their sense of humour. I would also like to thank the committee members, Professor Paul Major, Dr. Hollis Lai, and Dr. Ivonne Hernandez, for their assistance and support. In addition, special thanks to Dr. Hollis Lai for his statistical guidance. Moreover, I am grateful to Dr. Neel Kaipatur for allowing me to utilize his sample.

My neighbour Duncan and his lovely wife Maxine Galloway have been very helpful and supportive throughout my time in Edmonton. Thank you for assisting me with snow removal, lawn cutting, and transportation while my vehicle was inoperable. You made my stay in Edmonton comfortable and delightful. Additionally, I appreciated your support and lovely comments when my mood was down. This work would not have been possible without the cooperation of the technicians, assistants, and colleagues at the University of Alberta- school of dentistry. Thank you for your help.

I would like to thank my family, mentors, and friends for their support throughout my study. I would also like to thank my wife, Dr. Rand Al Ramahi, for her persistent encouragement and support during my study time and my kids, Mohammad and Yusuf, for making my life enjoyable. All thanks to my mother and father for their prayers.

Finally, I want to express my gratitude to all patients who willingly participated in this research.

## Table of Contents

LIST OF TABLES .....	IX
LIST OF FIGURES .....	X
Chapter 1: Introduction .....	1
1.1 Statement of the problem .....	1
1.2 Aims .....	2
1.3 Hypothesis .....	3
1.4 Research questions .....	3
Chapter 2: Literature review .....	5
2.1 Anatomy of the Temporomandibular joint (TMJ).....	5
2.2 Embryology of the Temporomandibular joint (TMJ) .....	10
2.3 Developmental changes of the Temporomandibular joint (TMJ).....	12
2.4 Functional appliances and class II Malocclusion .....	17
2.4.1 Herbst appliance .....	20
2.4.2 Xbow appliance .....	21
2.4.3 Proposed Effect of Herbst and Xbow Appliances on the TMJ .....	22
2.4.4 Radiological Evaluation of the TMJ Post Herbst and Xbow appliances .....	25
Chapter 3: Materials & methods; Research methodology and measurements method of the landmarks displacement through-plane reconstruction technique; Intra-rater reliability design .....	26
3.1 Research Methodology .....	26
3.1.1 Objectives of this research .....	26

3.1.2 Study Sample Overview and Blinding .....	27
3.1.3 Participant Selection .....	27
3.1.4 Study Groups .....	28
3.1.5 Clinical significance .....	31
3.1.6 Stopped trial .....	33
3.1.7 Interim analyses and stopping guidelines .....	33
3.2 Generation of three-dimensional ortho-slice and iso-surface of the TMJ, cranial base, and face from CBCT images to assess landmarks using AVIZO© software .....	33
3.2.1 Software dissertation .....	33
3.2.2 Generation of the planes and measurement of the perpendicular distance from each landmark to each plane (Sagittal, Axial, and Coronal) .....	34
3.2.3 Study population and data collection for the measurements of the landmarks for pre-research intra-reliability testing .....	35
3.2.4 The hypothesis of intra-rater reliability .....	45
3.2.5 Intra-rater reliability design .....	46
3.3 Statistical methods .....	47
3.3.1 General overview .....	47
3.3.2 Description of statistical analysis .....	48
3.3.3 Ethical approval .....	53
Chapter 4: Results; Intra-rater reliability analyses; Measurements of the landmarks positional change of the TMJ .....	55
4.1 Intra-Rater Reliability .....	55
4.1.1 Intra-rater reliability results of landmark points .....	55

4.1.2 Intra-rater reliability results in the distance from each reconstructive plane to the condylar and glenoid fossa landmarks .....	58
4.2 Results of the research .....	59
4.2.1 Losses and exclusions .....	59
4.2.2 Participant flow .....	60
4.2.3 Pre-MANOVA assumption tests .....	62
4.2.4 One-way MANOVA test for all landmarks jointly, condylar landmarks, and fossa landmarks corresponding to each dimension (anteroposterior, vertical and mediolateral) .....	64
Chapter 5: Discussion and conclusions .....	68
5.1 Discussion of the study .....	68
5.1.1 Discussion of previous research limitations and methods implied in this thesis to overcome the previous limitations .....	68
5.1.2 Operator reliability and error .....	72
5.1.3 Condyle and fossa positional change .....	73
5.1.4 Clinical significance of our results .....	78
5.2 Future recommendations .....	78
5.3 Limitations .....	80
5.3.1 Machine limitation .....	80
5.3.2 Avizo© limitations .....	81
5.4 Conclusions .....	82
References .....	83
Appendix .....	101

## LIST OF TABLES

Table 2.1 Comparison between Herbst and Xbow appliances .....	24
Table 3.1 Landmarks to establish reference planes .....	37
Table 3.2 Landmarks definitions .....	39
Table 3.3 Landmarks of condyle and fossa .....	43
Table 4.1 Intraclass correlation coefficient (95% confidence interval) and p-value. Please notice that the values were rounded to the second decimal place except for the p-value .....	56
Table 4.2 Measurement error difference mean between landmarks (intra-joint distance in mm); and standard deviation (SD). Please notice that the values were rounded to the first decimal place in mm .....	59
Table 4.3 Descriptive analysis of age (years) and time interval duration (months).....	61
Table 4.4 Gender distribution among treatment groups .....	62
Table 4.5 Summary of nine MANOVA tests of multiple landmark settings means variation in positional change corresponding to each plane. Notice that the values were rounded to the second decimal place .....	67
Table A3.1 Measurement error difference average in each landmark relative to each plane in millimetre and standard deviation (SD) .....	104
Table A3.2 Measurement error average in each axis in millimetre and standard deviation (SD). Please notice that the values were rounded to the first decimal place in mm .....	106
Table A3.3 Variables representing landmarks corresponding to each plane of the groups .....	108

## LIST OF FIGURES

Figure 2.1 The Temporomandibular Joint: Lateral view .....	8
Figure 2.2 Herbst appliance.....	21
Figure 2.3 Xbow appliance .....	22
Figure 3.1 Xbow appliance; clinical photograph .....	29
Figure 3.2 Herbst appliance; clinical photograph .....	30
Figure A2.1. Summary information about AVIZO LITE© Berlin, Thermo Fisher Science 2019 .....	101
Figure A2.2 Sample size calculation .....	102
Figure A2.3 The formulas and methodology for generation of the planes and measuring the orthogonal distance from each landmark to each plane (Sagittal, Axial, and Coronal) .....	103
Figure A3.1 Boxplots of all dependent variables (mean difference in distance of the 12 landmarks between T0 and T1 timelines corresponding to each plane) in each group (control, Herbst and Xbow) .....	118
Figure A3.2 Scatterplot matrices of each pair of dependent variables (mean difference in distance of the 12 landmarks between T0 and T1 timelines corresponding to each plane) in each group (control, Herbst and Xbow) .....	120
Figure A3.3 Matrices that express hypotheses of each MANOVA test .....	122

# **Chapter 1: Introduction**

## **1.1 Statement of the problem**

Clinicians need to understand the effect of oral functional appliances such as the Herbst and Xbow on the osseous structure of the temporomandibular joint (TMJ). The potential detrimental effects to the TMJ associated with these appliances which alter the postural position of the mandible in growing patients needs to be understood. Furthermore, the orthodontist must understand the mechanism by which these appliances achieve correction of Class II malocclusion.

Patients with Class II malocclusion and pre-treatment symptoms of temporomandibular disorders (TMD) of muscle origin seemed to gain more from orthodontic treatment regarding their functional outcomes (Henrikson, 1999). Orthodontic appliances that alter the postural position of the mandible may result in osseous remodeling with anterior displacement of the condyle and fossa (LeCornu et al., 2013).

According to Lecornu et al., anterior positional advancement of the mandible achieved using the Herbst appliance may promote mandibular development, modify the growth, and alter the location of the condylar/fossa (LeCornu et al., 2013). Whether the condyles reestablish centric position inside the glenoid fossa after finishing the Herbst appliance is debatable. When Herbst appliance is utilized, it may result in a change in the morphology of the TMJ. This change may be induced by a remodelling process of the glenoid fossa and condyle, which may influence the position of the condyle and the articular disc (Voudouris et al., 2003). The researchers pointed

out that there is debate over the extent to which these effects are produced by skeletal as opposed to dentoalveolar changes.

On the other hand, Flores-Mir et al. evaluated the skeletal and dental effects of the Xbow appliance using cephalograms to determine effectiveness. They concluded that the Xbow appliance does not provide clinically significant mandibular advancement. The overjet correction was created by dental movement rather than the skeletal movement of teeth (Flores-Mir et al., 2009). This may be attributed to the Xbow appliance's freedom of movement which allows for forgiving retrusion of the mandible into centric occlusion during treatment as compared to the Herbst appliance (Flores-Mir et al., 2009).

It is crucial to recognize the possible effects of fixed functional appliances that might in advancing the mandible by remodelling the condyle or fossa. Furthermore, for the long-term viability of these treatments, we need to know how such a fixed functional appliance might influence condyle and fossa position. Understanding the effects of these appliances on the growing mandible is essential for clinical orthodontic treatment reliability and outcome.

## **1.2 Aims**

The primary objective of this study is to evaluate three-dimensional positional changes in the condyle /and the glenoid fossa relative to the reference planes utilizing different Class II fixed mandibular positioners/appliances (Herbst and Xbow) compared to controls.

The secondary objective is to compare three-dimensional positional changes of the condyle /and the glenoid fossa within and between the groups regarding the type of treatment (Herbst versus Xbow; Herbst versus control; and Xbow versus control), gender, age, and timeline duration covariances; If significant differences are found from the primary objective.

### **1.3 Hypothesis**

Herbst group will show significant condylar and glenoid fossa remodelling and positional change post treatment than the Xbow and control group because the mandible protrudes forward from the glenoid fossa in the case of the Herbst appliance. Because of the Xbow appliance's freedom of movement, the jaw may be retracted into centric occlusion in contrast to the Herbst appliance (Flores-Mir et al., 2009), which may not contribute to remodelling.

### **1.4 Research questions**

The following were the preliminary investigations in this study design:

- Skeletal positional change (in each dimension) of the TMJ (condyle and fossa) resulted from appliance intervention.

In this research, the variable of interest was the mean displacement of the condyle and glenoid fossa of TMJ relative to reconstructed planes as a consequence of therapy. As a result, this study addresses two research questions, which are:

- Are there any significant differences between Class II mandibular positioners/appliances (Herbst and Xbow) and the control group in the condyle/and glenoid fossa position in each dimension between T0 and T1?

- If significant differences are found, does the type of appliance, gender, age, and timeline duration make a difference in the condyle and glenoid fossa position in each dimension?

## **Chapter 2: Literature review**

### **2.1 Anatomy of the Temporomandibular joint (TMJ)**

The temporomandibular joint (TMJ) is a synovial junction that connects the mandible's head (condyle) to the glenoid fossa on the undersurface of the temporal bone's squamous part (Sinnatamby, 2011). The TMJ comprises a disc, articular surfaces, joint capsule, synovial fluid, synovial membrane, cartilage, and ligaments. The cranial surface of the TMJ is formed from the temporal bone's squamous part. The glenoid fossa is the concavity that runs along the surface of this bone. The posterior articular ridge is the posterior part of the glenoid fossa. The postglenoid process (PGP) is a laterally based protrusion off of this ridge. The posterior part of the glenoid fossa also contributes to the external auditory meatus' superior wall (Bag et al., 2014).

The condyle is a convex articular surface in contact with the articular disc of the TMJ. The dimension of the condyle ranges from 8-10 mm anteroposteriorly, 15-20 mm mediolaterally, and 17-18 mm superio - inferiorly (Al-Koshab et al., 2015; Alomar et al., 2007).

These joints are unique in that they are bilateral joints that function as one unit. Since the TMJ is connected to the mandible, the right and left joints must function together and therefore are not independent of each other.

The articular eminence (AE) forms the anterior border of the glenoid fossa. The AE is a transverse bony prominence medial to the zygomatic process's posterior border. The articular tubercle is a tiny bony ridge located on the lateral area of the AE, where it meets the inferior aspect of the root of the zygomatic process. The lateral collateral ligament attaches to this tubercle. The glenoid fossa's lateral edge is somewhat elevated. It curves medially anterior to posterior till it reaches the postglenoid process (PGP) (Bag et al., 2014). The caudal articular surface is the mandible's cephalic side. It is formed by an ovoid condylar process of 15–20 mm broad transversely and 8–10 mm wide anteroposteriorly (Alomar et al., 2007). The mandible is a single bone with a horseshoe-shaped body connected by a pair of vertical rami at the posterior ends. Each of which is topped by a head or condyle. The skull, with which the mandible articulates, is likewise a single component mechanically, with each side having a glenoid fossa. This complex functions as a single functional joint, as movement at one TMJ is impossible without concurrent movement at the opposing joint. Thus, the TMJ forms the craniomandibular articulation's bilateral component (Sinnatamby, 2011).

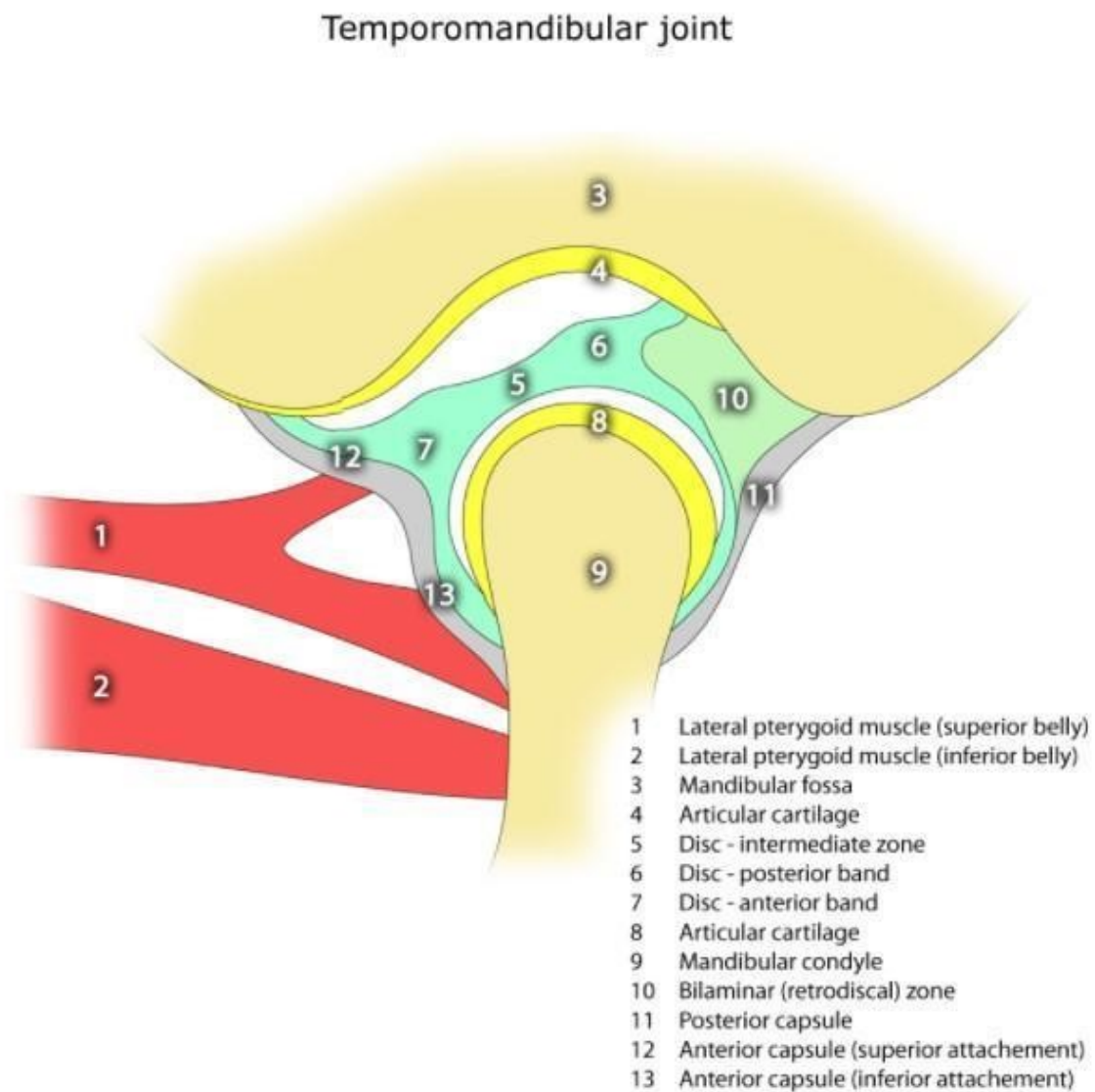
The articular disc, positioned between the condyle and the glenoid fossa, contains biconcave surfaces and is round or oval. Furthermore, the disc has three bands: an anterior band, a narrow middle zone, and a posterior band. The superior layer adheres to the PGP and prevents the disc with a significant mandibular depression from sliding. The inferior part of the disc prevents the disc from rotating excessively around the condyle. The anterior part of the disc is connected to the joint capsule, condylar head, AE, and superior belly of the lateral pterygoid muscle. The posterior band links to the bilaminar retro-discal tissue posterior to the condyle within the

glenoid fossa, connecting the condyle and temporal bone. The disc's medial and lateral surfaces are securely connected to the condyle (Aiken et al., 2012).

The capsule is attached anteriorly high on the mandible's neck, near the articular edge, but posteriorly lower on the neck. It is anteriorly attached directly in front of the temporal bone's articular eminence (Figure 2.1), posteriorly to the squamotympanic fissure, and medially and laterally to the glenoid fossa borders. It is loose above the disc and taut beneath the disc.

Additionally, the fibrocartilaginous disc within the joint divides it into upper and lower cavities (Figure 2.1). Both bone surfaces are coated in the same fibrocartilage as the disc. Though referred to as fibrocartilage, the articular cartilage and disc are primarily composed of collagen fibres and contain very few cartilage cells (Sinnatamby, 2011).

Figure 2.1 The Temporomandibular Joint: Lateral view (Gaillard F, 2011).



Apart from the teeth' stabilizing function, the prominence of the articular eminence and contraction of the posterior temporalis fibres inhibit forward movement of the condyle, while the lateral ligament fibres and contraction of the lateral pterygoid prohibit backward movement. The joint is less stable in the open than close position because the condyle is forward on the slope of

the articular eminence. The most prevalent displacement type is anterior dislocation (Sharma et al., 2015). The articular eminence, the lateral ligament, masseter, temporalis, and medial pterygoid muscles oppose forward dislocation. The joint receives nerve supplies from the auriculotemporal and masseteric nerves (Sinnatamby, 2011).

At the TMJ, there are three distinct sets of mandibular movements. These include depression and elevation motions (opening and shutting the jaws), side-to-side movements (lateral excursion) and protrusion and retraction (protrusion and retrusion). The muscles typically referred to as mastication muscles—temporalis, masseter, medial and lateral pterygoids—play a significant role in these motions; others involved can be referred to as supplementary mastication muscles (Sinnatamby, 2011). For decades, anatomists have believed that the lateral pterygoid muscle is formed by two distinct heads—inferior and superior—with the superior head mainly inserted into the condyle (Carpentier et al., 1988). However, it has been hypothesized that the two heads of the lateral pterygoid muscle may form two different muscles. This suggestion may be supported because each head's nerve supply and function are unique (Bhutada et al., 2008; D'Ippolito et al., 2010). Recent investigations have confirmed the existence of two/or three distinct muscle insertions of the superior head of the lateral pterygoid muscle (Antonopoulou et al., 2013; Omami & Lurie, 2012). Omami & Lurie have suggested two types of insertions of the superior head of the lateral pterygoid muscle. Type I, in which the attachment of the superior head is exclusive to the disc.

On the other hand, the superior head is connected to the disc-condyle complex in type II (Omami & Lurie, 2012). Antonopoulou and colleagues suggested three types of insertions of the superior head of the lateral pterygoids muscle. In type I, the superior head of the lateral pterygoid muscle is inserted into the condyle and disc-capsule complex. The superior head of the lateral pterygoids muscle is exclusively attached to the condyle in type II. The superior head of the lateral pterygoids muscle is attached exclusively to the disc-capsule complex in type III (Antonopoulou et al., 2013). The lateral pterygoids muscle is functionally diverse, with its heads exerting a range of actions on the condyle–disc complex (Bhutada et al., 2008). It is suggested that specific insertions types and muscle dysfunction may create an inherent susceptibility for TMJ internal derangement (Taskaya-Yilmaz et al., 2005). However, anterior disc displacement explained by the superior head of the lateral pterygoids muscle attachment type is improbable; the type of muscle insertion does not seem to be predictive or prognostic of TMJ internal derangement (Dergin et al., 2012; Omami & Lurie, 2012).

## **2.2 Embryology of the Temporomandibular joint (TMJ)**

The embryonic growth of the TMJ is similar across mammalian species but is markedly different from other synovial joints (Li et al., 2015). Unlike long bone joints, which grow from a single skeletal condensation, the TMJ develops from two discrete and widely separated mesenchymal condensations: the glenoid fossa blastema and the condylar blastema (Li et al., 2014).

The embryologic development of the TMJ is defined by three stages: blastemic, cavitation, and maturity. The blastemic stage begins at approximately 7 to 8 weeks of gestation (Mérida-Velasco

et al., 1999). Two mesenchymal blastemas are produced. They originate from neural crest cells in the first branchial arch, which form the temporal bone and mandibular condyle. The glenoid fossa blastema develops from the otic capsule and is ossified by a transmembranous ossification (Wang et al., 2011). The condylar blastema soon develops into a rectangular cell condensation lateral to and above Meckel's cartilage and is then connected medially by the lateral pterygoid muscle. Simultaneously, the condylar blastema develops from the mandible's secondary condyle cartilage and undergoes endochondral ossification, eventually expanding anterior/medially (Mérida Velasco et al., 2009).

A thick band of mesenchyme is between the two blastemas that begin to compress and create the future articular disc. Before the articular disc separates the TMJ into two compartments, mesenchyme develops between the glenoid fossa, and condylar blastemas condense (Yokohama-Tamaki et al., 2011). As the condyle ascends superiorly, the mesenchyme divides into layers of fibrous tissues, eventually dividing the upper and lower compartments (Gu et al., 2014). The compressed mesenchyme between the two blastemas develops into several layers of fibrous tissue, which eventually separates into the upper and lower synovial layers of the future disc during the cavitation stage (Mérida-Velasco et al., 1999).

From 12 weeks' gestation through delivery, the maturation stage occurs. At 17 weeks, the joint capsule becomes apparent, and the intervening cartilage becomes evident at 19 to 20 weeks. At 26 weeks, the cellular and synovial tissues continue to differentiate. The glenoid fossa and

condyle developments are affected by surrounding vascular ingrowth and muscular pressure forces (Tamimi D & Hatcher DC, 2016).

Development of the soft tissues surrounding the joint occurs synchronously with the TMJ's skeletal components (Loughner et al., 1997). After the conclusion of cavitation, the TMJ displays significant ossification. Moreover, during the condyle and glenoid fossa development, functional modification of the articular disc results from the avascular event, and significant condensation of the articular disc occurs (Owtad et al., 2011). Furthermore, the joint capsule serves to enclose the joint bone prominences and the articular disc, and the development of the muscles and ligaments is continued throughout the development of the joint (Yamaki et al., 2005).

### **2.3 Developmental changes of the Temporomandibular joint (TMJ)**

The cartilage of the TMJs has secondary cartilage in contrast to the other joints, which have primary cartilage (Wadhwa & Kapila, 2008). This secondary condylar cartilage is a crucial growth center responsible for ideal growth potential concerning the craniofacial skeleton compared to the articular cartilage seen in other joints (Bender et al., 2018). Secondary cartilage forms in conjunction with certain bones created by intramembranous ossification after the bones have already developed. Intramembranous ossification is in contrast to endochondral ossification, in which the cartilage forms before the bone and is referred to as primary cartilage. Primary cartilage formation starts in the cartilage cells of the epiphyseal plate's core layer. Cells undergo mitosis at this developmental stage. Moreover, the two daughter cells will carry the whole of the parent cell's genetic information. The two daughter cells then expand to the parent's

size during the following phase of epiphyseal growth. Each cell generates and secretes an extracellular matrix, which causes cells to disperse and enter many paths.

The cells may differentiate into new progenitor cells or be replaced by bone. One of the critical characteristics of primary cartilage formation occurs in the central portion of a long bone's epiphyseal plate. Interstitial growth occurs when new tissue forms inside old tissue (Garant P, 2003). Secondary condylar cartilage formation starts with undifferentiated mesenchymal cells covering the prenatal or postnatal condyle. Mesenchymal cells divide throughout their early phases to become increasingly smaller cells but finally reach their maximum size. These mesenchymal cells move into the inner condyle and the cartilage, differentiating into immature cartilage cells (Garant P, 2003). The cartilage develops through mesenchymal tissue differentiation rather than mitosis of cartilage progenitor cells. Appositional growth refers to growth from outside (Shen & Darendeliler, 2005).

Unlike other synovial joints, the TMJs articular surfaces of the TMJ are composed of fibrocartilage instead of hyaline cartilage. One of fibrocartilage's distinguishing properties includes type I and type II collagens, in contrast to hyaline articular cartilage, which has type II collagen (Mizoguchi et al., 1992). Fibrocartilage in the TMJ has the following benefits over hyaline cartilage: the fibres are densely packed and can bear movement stresses; it is less vulnerable to the effects of ageing; it is less prone to break down over time; and it has a tremendous potential to heal (Bergman AA & Heidger PM, 1996). Moreover, fibrocartilage is more resistant to shear pressures than hyaline cartilage, making it a preferable material for

withstanding the high occlusal stress exerted on the TMJ (Milam, 2005). On the other hand, factors such as sex hormones that lead to degenerative changes may target fibrocartilage differently from hyaline cartilage (Park et al., 2019).

At birth, most condylar cartilage is replaced by bone through endochondral ossification; however, the cephalic part of the condylar cartilage remains until maturity. Moreover, the condylar cartilage loses its thickness and vascularity with ageing (Smartt et al., 2005; Tamimi D & Hatcher DC, 2016). At the time of birth, the glenoid fossa of the TMJ is flat. Over time, the fibrous connective tissue changes into fibrocartilage (Smartt et al., 2005). The condylar cartilage provides a stable relationship to the temporal bone throughout development, while the mandible grows downward and forward (Kozak FK et al., 2015).

There are two phases of growth spurts: 5-10 years of age and between 10 and 15 (Smartt et al., 2005). The secondary condylar cartilage is a significant development site for the TMJ and serves as the craniofacial skeleton's primary growth centre (Kozak FK et al., 2015). Posteriorly, superiorly, and laterally, the condyles grow (Smartt et al., 2005). Within the first three years of life, fast lateral development of the mandible occurs via symphyseal ossification and growth of the condyles in both the posterior and superior directions, enabling the ramus to expand in height (Tamimi D & Hatcher DC, 2016). At birth, the articular eminence has a moderate slope, and its final shape is entirely functionally determined by force generated by the masticatory muscles and teeth (Tamimi D & Hatcher DC, 2016). These pressures have shaped the articular eminence to about half of its adult form by the age of three, which is almost complete by twelve years

(Tamimi D & Hatcher DC, 2016). After three years of age, significant bone remodelling occurs over the whole mandibular surfaces. Although the mechanism of this process is unknown, it may be governed by main development centres inside the mandible and response to external mechanical pressures. The surrounding biomechanics is considered a driving factor in morphology and bone deposition stimulation (Smartt et al., 2005).

In general, bone apposition occurs along the condyle, coronoid, alveolar process, posterior edge of the ramus, and buccal/labial surface of the mandible. In contrast, bony resorption occurs along the anterior edge of the ramus and usually along the mandible's lingual side (Krarup et al., 2005). There is periosteal resorption and endosteal deposition at the condylar neck and ascending ramus, giving the jaw a more acute angle. At about 5 to 6 years of age, the mandible's body and ramus begin to develop in proportion to the craniofacial bone, which corresponds with the first mandibular growth spurt (Smartt et al., 2005). Mandibular width is determined throughout early adolescence (Tamimi D & Hatcher DC, 2016). Females complete their mandibular growth two to three years after menstruation, whereas males complete their mandibular growth approximately four years after sexual maturity (Smartt et al., 2005).

Several studies noted variation in the condylar position related to the occlusion (Rodrigues et al., 2009a, 2009b). The shape of the TMJ is greatly affected by the function and the type of occlusion. Even in the same individuals, the condylar shape and form can be different from side to side. Condylar variation might result from variability in demands needed to perform masticatory and other functional activities (Rodrigues et al., 2009a, 2009b). Krisjane et al.

observed a statistically significant difference between Class II and Class III patients utilizing CT scans of the condyle's height, glenoid fossa's width, and condylar process (Krisjane et al., 2009).

Mandibular and TMJ trauma are a significant cause of TMJ disorders and associated pain (Defabianis, 2001, 2003). The bony components (the condyle and fossa) and the accompanying fibrocartilage surfaces, synovial lining, and the articular disk are among the structures that might be injured. A healthy masticatory system is perhaps the most crucial factor in TMJ remodelling; if a TMJ exhibits internal derangement, adaptive or even fractured condyle, the function might be affected, especially in growing patients (Defabianis, 2003). The condyle is the bedrock of mandibular shape and function. The jaw's growth and occlusion development also depend on the condyle's robustness (Dimitroulis, 1997). As a result of TMJ trauma, facial asymmetry, malocclusion, developmental abnormalities, osteoarthritis, an ankylosis might develop (Defabianis, 2003). The significance of the condyle as an adaptive growth center seems to be supported by clinical research, as well (Kozak FK et al., 2015). Such an injury could alter the growth and development of the mandible. However, the probability of TMJ dysfunction seems to be linked to the increasing age of the growing patient at the incident of injury (Dimitroulis, 1997). Studies that demonstrate degenerative change following TMJ injury are well documented (Dimitroulis, 1997; Seligman & Pullinger, 1996; Yun & Kim, 2005). Clinical evidence of acute synovitis, including fibrillation and ecchymosis, was seen during the arthroscopic evaluation of mandibular fractures that did not directly involve the condyles. Additionally, cytological and biochemical investigation of these patients' synovial fluids revealed the presence of degenerated cells, inflammatory cells, crystals, and a significant number of pain-related mediators, including prostaglandin E2 and leukotriene B4 (Yun & Kim, 2005). Additionally, several clinical research

studies have shown that a trauma history is a distinguishing factor in individuals with intracapsular TMJ dysfunction (Seligman & Pullinger, 1996).

## **2.4 Functional Appliances and Class II Malocclusion**

Class II malocclusion is a common orthodontic problem, affecting about 30% of the general population (McLain & Proffitt, 1985). Functional appliances have been in practice for many years and are commonly used to correct a mandibular deficiency (functional class II correctors). Generally speaking, the fundamental distinction between fixed and removable functional appliances is that compliance is prioritized with removable devices, while full-time wear is ensured with fixed devices (Dandajena, 2010). Furthermore, fixed appliances maintain device positioning and create substantial bite advancement while allowing a limited amount of vertical mouth opening (Shen et al., 2005). On the other hand, these appliances have a higher risk of breakages and a higher number of emergency calls (O'Brien et al., 2003). While compliance with fixed functional appliances is less critical, they may be less forgiving in other ways, requiring greater chairside and laboratory time and being more prone to mechanical failure (O'Brien et al., 2003). However, the improvement of fixed functional appliances, especially the more flexible types, allows for more mobility in mandibular excursions including protrusion, improving patient comfort (Shen et al., 2005). On the other hand, removable appliances may provide excessive vertical mouth opening. However, they might interfere with function and mandibular mobility, making them less effective for cases that need long-standing treatment (Shen et al., 2005).

Concerning fixed functional appliances, they are subdivided into three categories: fixed rigid, fixed flexible, and fixed hybrid (Ritto & Ferreira, 2000). Fixed rigid variations, such as the Herbst appliance, fixed twin block, and mandibular anterior repositioning appliance (MARA), have a rigid active component. The Herbst appliance has been hypothesized to have both skeletal and dentoalveolar effects (Pancherz, 2003). The Jasper Jumper is one of the members of the fixed flexible group. A fixed hybrid functional appliance falls between rigid and flexible appliances, with a spring giving the device flexibility. Examples are the Forsus Fatigue device and the Twin Force bite corrector (Dandajena, 2010). When hybrid appliances are used with headgear, these devices may provide consistent sagittal forces, especially while the mouth is closed (Oztoprak et al., 2012).

The goal of the mandibular advancement functional appliances is to enhance mandibular advancement by correcting underlying structural anomalies (LeCornu et al., 2013). Some postulated that the condyle could be mobilized to a new position, inducing morphological and positional changes through adaptation and remodelling utilizing protrusive appliances (Katsavrias, 2003). The fixed functional device anteriorly shift the condyles, which may result in adaptive forward remodelling of the glenoid fossa. However, the degree to glenoid fossa remodeling with functional appliances aid in class II correction is debatable (LeCornu et al., 2013). Kinzinger and colleagues performed a study using magnetic resonance imaging (MRI), and they found that both joints returned to their pre-treatment condylar-fossa relationship following fixed functional orthodontic treatment. They postulated that the improved occlusion was not obtained by repositioning the TMJ. This postulation might suggest dentoalveolar

adaptation rather than skeletal remodelling. However, their investigation solely included Functional Mandibular Advancers (FMA) appliances (G. Kinzinger et al., 2007).

Patients treated with Herbst or Xbow appliances usually have class II malocclusion or sagittal skeletal deficiency related to their functional mandible appliances, such as Herbst and Xbow's effect on the osseous structure of the TMJ is debated, especially with growing patients where growth and remodelling are likely to occur during orthodontic treatment. Henrikson concluded that patients with class II malocclusion with TMD might benefit functionally from orthodontic correction of class II malocclusion. Such additive benefit could improve the patient's comfort without additive risk of worsening the temporomandibular symptoms (Henrikson, 1999).

Baltromejus and coworkers performed a study comparing activators to Herbst appliances. Their main objectives were to investigate condylar remodelling, glenoid fossa remodelling, and condylar position changes within the fossa. They found vertical and sagittal changes in the Activator group and a sagittal change (posterior) in the Herbst group (Baltromejus S et al., 2002). Souki et al. concluded that immediate forward displacement of the mandible occurred following wear of the Herbst appliance. They explained this change by bone remodelling of the condyles and rami compared to the matched Class II patients with other non-orthodontic dental treatments (Souki et al., 2017).

In an animal study, Chayanupatkul et al. performed early and late tissue sections on Sprague-Dawley rats. The temporomandibular remodelling was investigated using bite jumping devices at

an early (30 days) and late phase (44 days). These groups were compared to a natural growth group (matched control animals sacrificed at different time points). Their results showed that the early group presented less bone formation than the latter in the condylar sections. Regarding the glenoid fossa, bone formation was similar to that of the controls, either in the early or late group. They found that early appliance removal was associated with suboptimal posterior condyle growth but average glenoid fossa growth. They postulated that extending the duration of mandibular advancement ensures that mandibular growth returns to normal levels after treatment (Chayanupatkul A et al., 2003).

#### **2.4.1 Herbst Appliance**

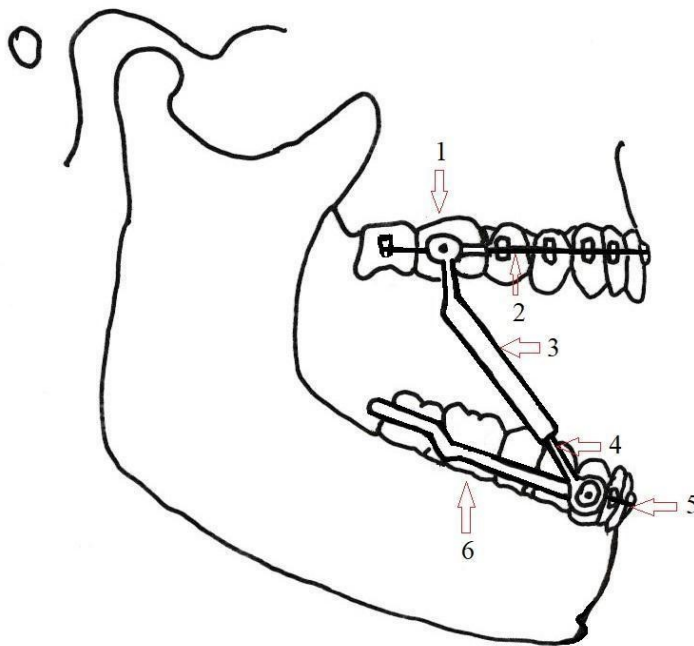
The Herbst appliance acts like a bilateral artificial joint that connects the mandible to the maxilla. The plungers, which act as a sliding radio-antenna inside a tube, sustain the mandible in a protruded position (Figure 2.2). This telescoping frame is attached to orthodontic bands placed on the permanent first maxillary molars and mandibular first premolars or canines. The horseshoe-type lingual arch connects the molars to premolars in each dental arch. The telescope can be extended gradually by applying a small ring (from 1.0 to 7.0 mm). The joints provide free mandibular opening but with sustained mandibular protrusion. It is worth mentioning that the original Herbst appliance design provides little lateral and no posterior freedom of movement, in contrast to the Xbow appliance (Papadopoulos MA, 2006).

Indications for using Herbst appliances may include skeletal class II malocclusion in young patients (Papadopoulos MA, 2006). Moreover, it may benefit patients diagnosed with anterior

disc displacement of the TMJ as disc recapture is observed in several cases (Pancherz et al., 1999).

Figure 2.2 Herbst appliance. 1&6: Crown over the molar; 2: Archwire; 3: Tube; 4: Sliding rod; 5: Bracket.

### Herbst Appliance

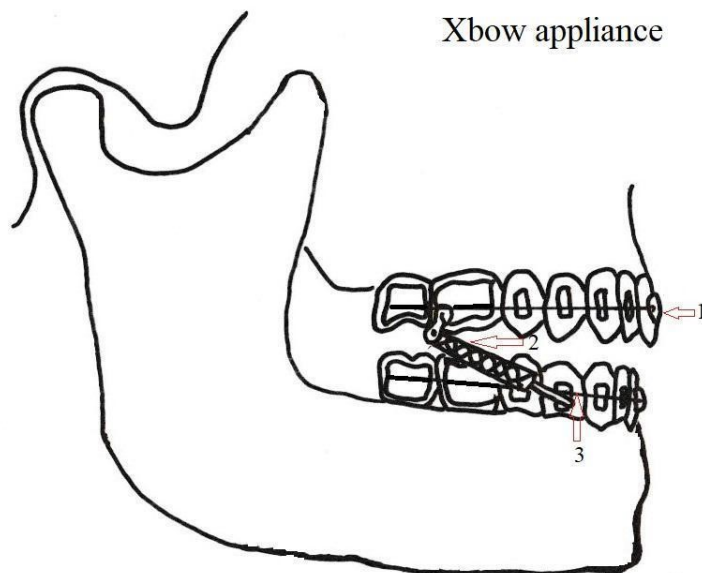


#### 2.4.2 Xbow Appliance

The Xbow appliance is a fixed appliance indicated for class II malocclusion (Figure 2.3). It comprises a lower arch labial and lingual bow, while an upper arch hyrax expands the maxilla. It is activated by a spring (Forsus fatigue resistant device (FRD)). This spring is attached to the

head tube of the maxillary first molar band and envelops the labial bow, which is clogged by a lock in the mandibular canine area. The spring can be used unilaterally or bilaterally (Flores-Mir et al., 2009). The Forsus springs are not a rigid activator, unlike the plunger of the Herbst appliance. It applies forward displacement to the mandible but provides the patient with free movement to move the mandible to centric occlusion.

Figure 2.3 Xbow appliance. 1: Bracket; 2: Forsus fatigue resistant device (FRD); 3: Archwire.



### 2.4.3 Proposed Effect of Herbst and Xbow Appliances on the TMJ

The proposed mechanism for correction of Class II malocclusion with fixed functional appliances is downward and forward posturing of the condyle in relation to the glenoid fossa. (Cheib et al., 2016; LeCornu et al., 2013). Lateral displacement is negligible or non-significant

(Cheib et al., 2016). The forward and downward positioning of the condyles may result in increased growth along the posterior superior surface of the condyle. It may also result in bone remodeling with forward displacement of the glenoid fossa. (Pancherz & Michailidou, 2004). However, Popowich and Nebbe, in a review, reported insufficient evidence to support the conclusion that significant remodelling and adaptation of the glenoid fossa occurs (Popowich et al., 2003).

Concerning the proposed/ suggested rotation of the condyle by functional appliances, Cheib et al. did not find any significant clockwise or counterclockwise rotation of the condyle in correlation to the measured overjet and overbite after activating the Herbst appliance (Cheib et al., 2016). According to Lecornu et al., anterior positional advancement of the mandible utilizing the Herbst appliance can be attributed to manipulating mandibular growth or changes in the growth direction or condylar/fossa positional changes (LeCornu et al., 2013). Moreover, they indicated that the degree to which these effects are caused by skeletal versus dentoalveolar alterations is controversial, bringing the dentoalveolar changes as a possible compensating factor over skeletal change.

Regarding the Xbow appliance, Flores-Mir et al. investigated the short-term skeletal and dental effects of the Xbow appliance utilizing cephalograms. They concluded that the Xbow appliance does not provide a clinically significant mandible advancement but may provide some maxillary forward growth restriction with increased vertical dimension. Dental rather than a skeletal movement of teeth -such as mandibular incisor protrusion and mandibular molars mesialization-

was responsible for overjet correction (Flores-Mir et al., 2009). In contrast to the Herbst appliance this may be related to the Xbow appliance's freedom of movement, allowing a forgiving retrusion of the mandible into centric occlusion during treatment (Flores-Mir et al., 2009). Table 2.1 compares the difference between Herbst and Xbow appliances.

Table 2.1 Comparison between Herbst and Xbow appliances.

Highlight	Herbst	Xbow
Indication of treatment	Class II malocclusion (Cheib et al., 2016; LeCornu et al., 2013)	Class II malocclusion (Flores-Mir et al., 2009)
Type of appliance	Fixed rigid (Ritto & Ferreira, 2000)	Fixed hybrid- Forsus fatigue resistant device (FRD) (Ritto & Ferreira, 2000)
Freedom of movement	Allow less movement - little lateral and no posterior freedom of movement (Papadopoulos MA, 2006)	Allow more movement - allowing a forgiving retrusion of the mandible into centric occlusion (Flores-Mir et al., 2009)
Skeletal change	Probable skeletal effect (Pancherz, 2003)	Probable non-skeletal effect (Flores-Mir et al., 2009)
Dentoalveolar effect	Yes (Pancherz, 2003)	Yes (Flores-Mir et al., 2009)
Mesialisation in the mandibular molars following treatment	More (Insabralde et al., 2021)	Less (Insabralde et al., 2021)
Mandibular size and length	Probable significant increase (Insabralde et al., 2021)	None (Insabralde et al., 2021)
The labial inclination of the mandibular incisors following treatment	Significant (Insabralde et al., 2021)	Significant (Insabralde et al., 2021)
Maxillary incisors retrusion following treatment	Significant (Insabralde et al., 2021)	Less (Insabralde et al., 2021)

#### **2.4.4 Radiographic Evaluation of the TMJ Post Herbst and Xbow appliances**

Many studies involving the evaluation of Herbst's and Xbows were performed using two-dimensional cephalogram imaging (Baltromejus S et al., 2002; Flores-Mir et al., 2009). This imaging modality might not sufficiently elucidate the complex structures and the three-dimensional changes during growth and treatment (Durão et al., 2013). Furthermore, magnification error and poor landmarks reproducibility in cephalograms are significant issues that can compromise the reliability of such studies (Durão et al., 2013). In contrast to conventional 2-dimensional radiographs, cone-beam computed tomography (CBCT) or conventional computed tomography could offer more informative imaging with minimal or no magnification but relatively higher radiation exposure (Lagravère et al., 2008; Pauwels et al., 2015). Linear measurements might not be comparable across the cephalogram studies due to magnifications differences. Because of variations in magnification, distortion, and issues associated with patient placement, the validity and reliability of cephalograms are inferior to CBCT (Cheib Vilefort et al., 2019). Furthermore, most studies addressing the TMJ positional changes following Herbst/Xbow appliances have been carried out using two-dimensional (2D) cephalometric imaging, with the results still relying on a 2D assessment of the changes in the glenoid fossa or the condylar position of three-dimensional anatomical structure (Baltromejus S et al., 2002; Flores-Mir et al., 2009; Manfredi et al., 2001; Pancherz & Michailidou, 2004). CBCT provides volumes that are true representations of accurate anatomic linear measures (1:1) of three-dimensional anatomic components (Lagravère et al., 2008). CBCT scans demonstrate acceptable intra- and inter-assessor reliability when measuring distances on a stiff facial surface (Moerenhout et al., 2009).

## **Chapter 3: Materials & methods; Research methodology and measurements method of the landmarks displacement through-Plane reconstruction technique; Intra-rater reliability design**

### **3.1 Research Methodology**

#### **3.1.1 Objectives of this research**

Primary objectives:

- To evaluate the three-dimensional positional changes (anteroposterior, vertical, and mediolateral) in the condyle /and the glenoid fossa utilizing different Class II fixed mandibular positioners/appliances (Herbst and Xbow) compared to controls if any occur. Results to be measured from CBCT data.

Secondary objectives

- To compare the condyle /and the glenoid fossa's three-dimensional positional changes (anteroposterior, vertical, and mediolateral), if any, determined from the primary objective, between the groups (Herbst versus Xbow; Herbst versus control, and Xbow versus control). Results to be measured from CBCT data.
- To evaluate the condyle /and the glenoid fossa, three-dimensional positional changes (anteroposterior, vertical, and mediolateral) difference-if, determined from primary objectives - between the group's covariances, including age at the start of treatment, gender, CBCT acquisition timeline duration. Results to be measured from Cone-Beam Computed Tomography data.

In a pre-treatment and post-treatment setting, the relative orthogonal distance from a point to a reference plane (axial, sagittal, and coronal plane) will be utilized to perform these objectives. The time frame between the CBCT acquisition is usually around 12 months. However, this can not be assured until analysis of the data.

### **3.1.2 Study Sample Overview and Blinding**

This is a secondary study conducted on a prospective randomized controlled parallel-group trial performed at the University of Alberta, School of Dentistry, Orthodontic Graduate Clinic-Oral Health Clinic. This investigation was carried out using a single-blinded data collector. CBCT images were coded, ensuring investigator blinding during landmark identification. Because the treatment is visually distinct, treatment provider blinding was not possible. Randomization for study participant allocation into the study groups was done independently of the treating clinician. Each step of the data analysis was completed by the same researcher, TA. The investigator could not discern between T0 and T1 CBCT pictures visually. For this investigation, there was no data monitoring committee present.

Demographic data was provided to the study investigator after all CBCT measurements were recorded.

### **3.1.3 Participant Selection**

Participants who met the eligibility requirements had a Class II malocclusion and were between ten and sixteen years old. Both sexes were involved in the study. A total of 59 participants were included in the study. The sample size in this secondary investigation was determined using the

sample size equation described in Appendix (Figure A2.2). The following were the criteria for inclusion and exclusion of this research:

Inclusion Criteria:

- Class II malocclusion (at least end to end molar relationship)
- ANB angle  $\geq 4$  degrees
- Late mixed or early permanent dentition stage of dental development
- At least the first molar and first premolars erupted in the maxillary arch
- Age range 10-14 females and 11-16 males
- Overjet  $\geq 1$ mm
- Overbite  $\geq 1$ mm

Exclusion criteria:

- Syndromes
- Craniofacial anomalies
- Gingival recession below the cemento-enamel junction
- TMJ pathology
- Greater than 6 mm dental crowding
- Congenitally missing permanent teeth (not including the third molars)
- History of trauma to TMJ

### **3.1.4 Study Groups**

The patients were assigned to one of three groups:

- Xbow intervention (n=19) with about 12 months (T1) of Xbow (Figure 3.1) from Time 0.

- Herbst intervention (n=21) with about 12 months (T1) of Herbst (Figure 3.2) from Time 0.
- Braces intervention (n=19) control group received about 12 months (T1) of watchful waiting from Time 0.

The present study only evaluated changes from T0 to T1.

Figure 3.1 Xbow appliance; clinical photograph (Insabralde et al., 2021).



Figure 3.2 Herbst appliance; clinical photograph (Insabralde et al., 2021).



Full-field of view (FOV) CBCTs at medium resolution (0.3mm voxel size, 8 to 9 seconds and 13cm x 16cm FOV) were obtained before treatment (T0) and about 12 months following the treatments (T1). The patient was positioned with the occlusal plane parallel to the floor with the teeth lightly touching in maximum intercuspation. The CBCT machine manufacturer uses an i-CAT machine (i-CAT, Imaging Sciences International, Hatfield, Pa); the location is 8D, 126 Edmonton Clinic. CBCT files were coded by a research assistant and transmitted anonymously to the investigator via hard drive. TA then randomized the CBCT files through Microsoft Excel© by randomly rearranging the codes throughout the sheet. After all CBCT measurements were

obtained, the code was broken so the data could be analyzed according to the study group with the inclusion of demographic data.

### **3.1.5 Clinical significance**

Clinical significance is defined as the significance of practical therapy results. It would be essential to have information that might influence diagnosis or treatment plans. Typically, this can be accomplished by clinical knowledge. In a CBCT assessment of the posterior cranial base, Currie and colleagues investigated several anatomical structures in the posterior cranial base- correlating to other landmarks in the middle and posterior cranial fossa- and their growth throughout adolescence -between the mean age of 13.1- 14.6 years- in patients who received braces and maxillary expansion treatments. Though it was used to demonstrate the clinical importance of cranial base development and growth, Currie and colleagues determined that a value of 1.5 mm was clinically crucial with changes in CBCT landmarks (Currie et al., 2020). Additionally, Liberton et al., classified the reliability of landmarks to each axis on CBCT into three categories based on the standard deviation of variable points to reference points: highly reliable (standard deviation less than 1mm), reliable (standard deviation between 1 and 2mm), and unreliable (standard deviation greater than 2mm) (Liberton et al., 2019).

De Assis and colleagues assessed the mandibular rami and condyles one year following mandibular advancement surgery for positional alterations and remodelling (de Assis et al., 2010). They discovered that the condyle typically moves no more than 2 mm after surgery. Additionally, they disputed that their sample had symptoms of temporomandibular joint

disorders throughout a one-year follow-up period. Moreover, this slight positional displacement was maintained one year after surgery (de Assis et al., 2010). However, Cheib Vilefort et al. proposed that a clinically acceptable difference between groups would be condylar positional alterations of greater than 1 mm (Cheib Vilefort et al., 2019).

On the other hand, because a radiographic significance of a single point in CBCTs may be defined by the voxel size (0.3 mm in our scans), the total radiological significance between two objects in CBCT would be two voxel sizes (0.6 mm). A random sample of untreated French-Canadian adolescents was reviewed at ages 10 and 15 to illustrate condylar growth and remodelling (Buschang & Gandini Júnior, 2002). The change of reference points was compared. Their investigation showed that PR (point on the posterior condyle determined by the superior tangent of the ramal plane) demonstrated a total horizontal displacement of about 2.5 mm during five years of growth (0.5 mm/year on average) (Buschang & Gandini Júnior, 2002). Thus, the clinical significance of a therapy result in this thesis will be as the following:

Clinical significance (effect of treatment might be probable/threshold) = total radiological significant + growth potential without treatment (in 1 year). From the aforementioned, 0.6 mm + 0.5 mm = 1.1 mm.

The clinical significance value of more than 1.1 mm will be used in this thesis since this value might represent a threshold, in which beyond this, a value might represent a treatment effect incorporating radiological and growth effects.

### **3.1.6 Stopped trial**

The research was neither suspended nor terminated, and there was no intention of suspending it. However, due to the COVID-19 pandemic, this research was slowed down in data collection and analysis.

### **3.1.7 Interim analyses and stopping guidelines**

No intermediate analyses were performed or stopping recommendations planned for this research, and no stopping guidelines were implemented or planned for this study. All therapy approaches utilized in all groups are identical and extensively used in academic and non-academic orthodontic clinics (Baysal & Uysal, 2014; Flores-Mir et al., 2009; Insabralde et al., 2021; Pancherz, 2003; Pancherz et al., 1999; Popowich et al., 2003).

## **3.2 Generation of three-dimensional ortho-slice and iso-surface of the TMJ, cranial base, and face from CBCT images to assess landmarks using AVIZO© software.**

### **3.2.1 Software dissertation**

Using AVIZO LITE© Berlin, Thermo Fisher Science 2019, ortho-slice and iso-surface imaging were generated. The TMJ, cranial base, and face was created using CBCT raw images to analyze landmarks. For more information about AVIZO LITE©, see Appendix (Figure A2.1).

Avizo© was chosen for comparable past projects at this dental school; the interface is simple to use and requires less learning time than other applications. The above statement represents the author's subjective view.

Regarding Avizo© technical specifications, all landmarks were located using ortho-slice multi-planner tracing (utilizing sagittal, axial, and coronal planes) except for the infra-orbital foramen landmark. For ortho-slice tracing, the slice thickness was 0.3 mm and colormap ranged from -1000 to 1000. Iso-surface was used to trace the infra-orbital foramen bilaterally. The threshold used for iso-surface ranged from 100-400 with a shaded draw style. This technique was implied to incorporate bone window without soft tissue inclusion.

### **3.2.2 Generation of the planes and measurement of the orthogonal distance from each landmark to each plane (Sagittal, Axial, and Coronal)**

Using the point coordinates of three reference planes described in Table 3.1, Sagittal, Axial, and Coronal planes were generated utilizing mathematical functions in Microsoft Excel©. Three points (P1, P2, P3) are used to create a reference for each reference plane (Table 3.1). The formulas and methodology for the generation of the planes are illustrated in Appendix (Figure A2.3).

The orthogonal distance from each landmark (Table 3.3) located on each condylar side (medial, lateral, and posterior) and each glenoid fossa side (antero-lateral, postero-lateral, and medial) to each reference plane were calculated utilizing mathematical functions in Microsoft Excel©. The

formulas and methodology for the generation of the orthogonal distance from each landmark to each plane (Sagittal, Axial, and Coronal) are illustrated in Appendix (Figure A2.3).

### **3.2.3 Study population and data collection for the measurements of the landmarks for pre-research intra-reliability testing**

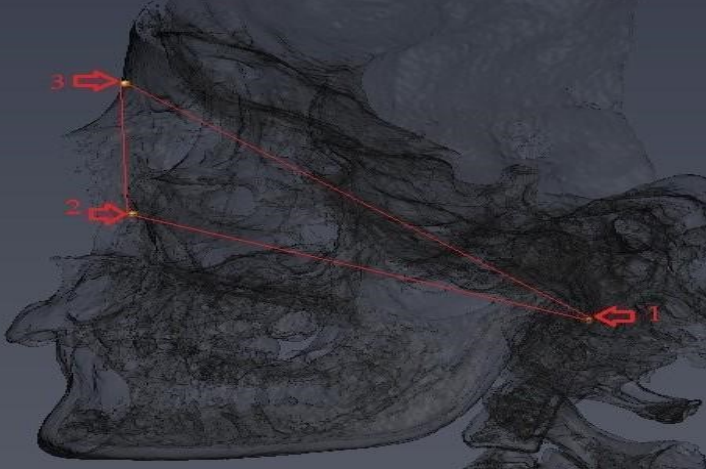
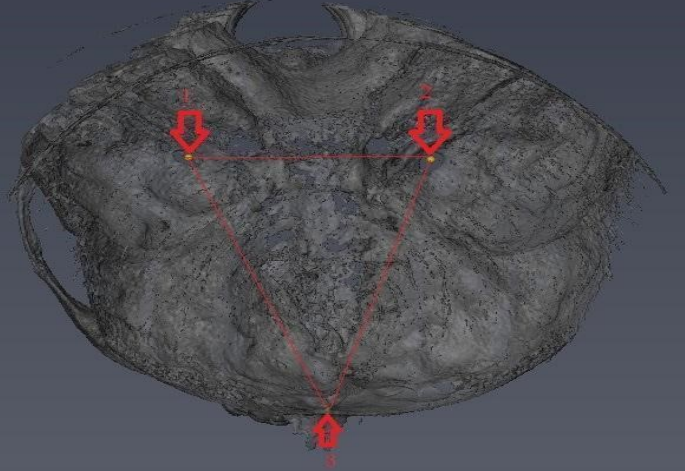
In Dentistry and Radiology, anatomic landmarks are often recognized, chosen for particular purposes, and utilized for assessing treatment changes and diagnosing problems throughout the treatment. Unquestionably, one must consider the possibility of mistakes to guarantee that landmarks are sufficiently reliable and dependable for their intended use (Liberton et al., 2019).

The identification of landmarks is a significant cause of measuring inaccuracy. Various variables may complicate the process of recognizing specific landmarks but are not limited to the clarity of the radiographs, landmark definitions, examiner's mistakes, instrumental and procedural errors (Mallya & Tetradis, 2014; Scarfe & Farman, 2014a, 2014b). Compared to typical 2-D imaging approaches, 3-D imaging has significantly minimized projection errors (Oz et al., 2011). These crucial elements influence a significant portion of the landmark selection process. Landmarks in this study were selected according to the following self-criteria (for intra-rater reliability testing):

- Easily located and accessible landmarks on Cone-beam Computed Tomography (CBCTs).
- Landmarks should be reproducible.
- Landmarks can be accurately defined.

- Three landmark sets were chosen: landmarks related to the cranial base and facial planes, condyle, and glenoid fossa landmarks.
- Proper representation of the field of interest (condyle, glenoid fossa, axial, coronal, and sagittal planes)
- Landmarks were classified into five categories: landmarks used for sagittal reference, landmarks used for axial reference, landmarks used for coronal reference, landmarks in the condyle anatomical structure, and landmarks in the glenoid fossa anatomical structure (Table 3.1&3.2).

Table 3.1 Landmarks to establish reference planes.

Landmark category	Landmark 1	Landmark 2	Landmark 3	Figure
Sagittal Plane Reference Landmarks	Foramen Magnum	Mid-point between Infraorbital Foramen	Nasion	
Axial Plane Reference Landmarks	Right foramen ovale	Left foramen ovale	Nasion	

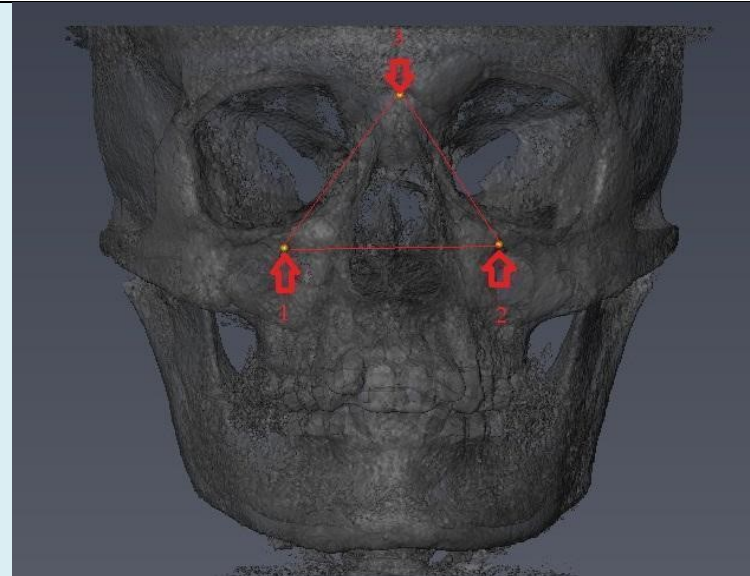
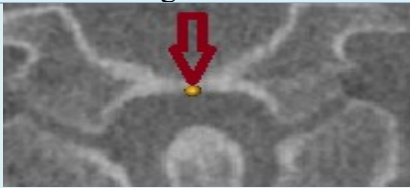
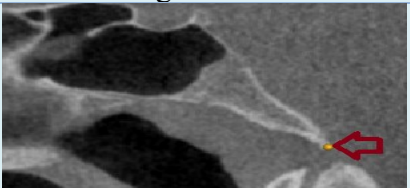
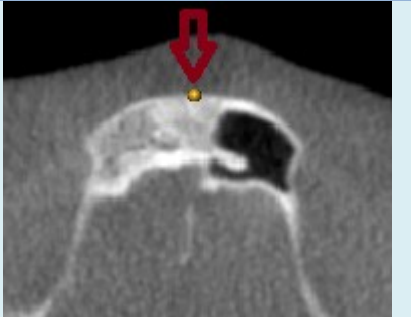
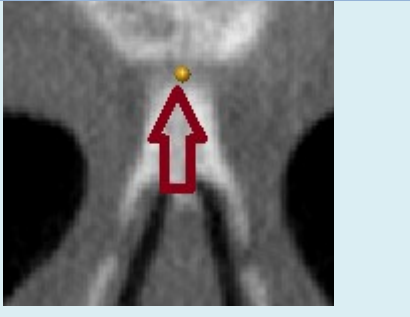
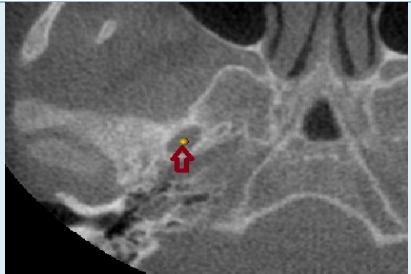
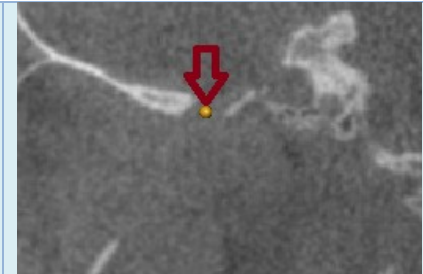
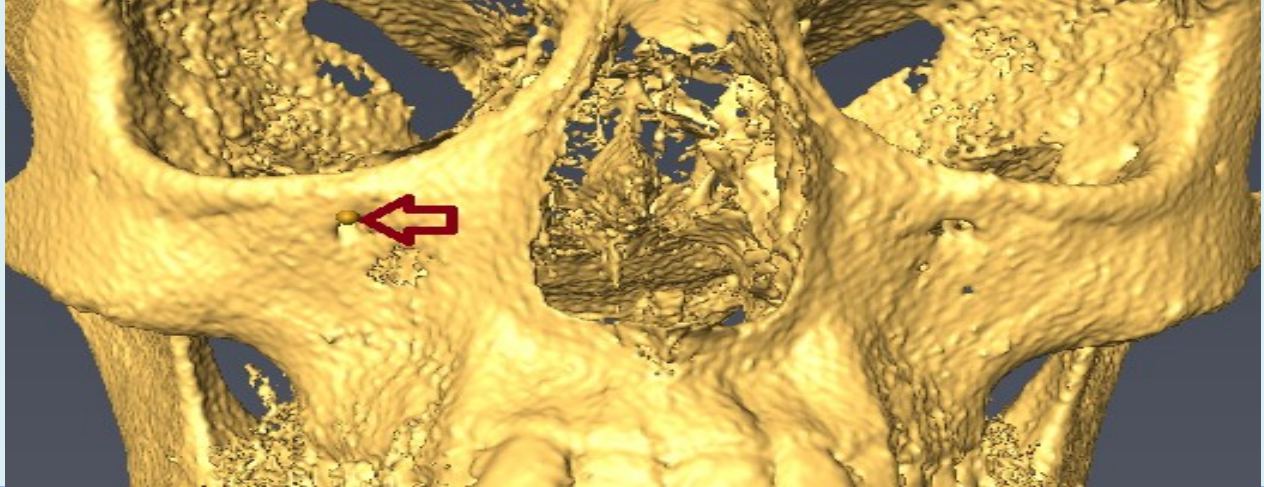
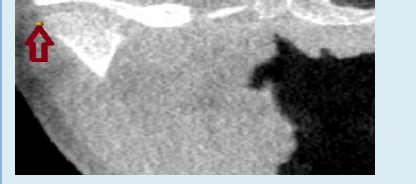
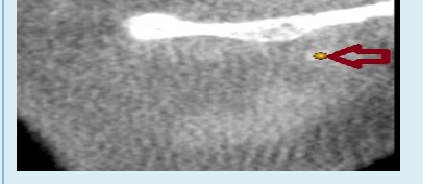
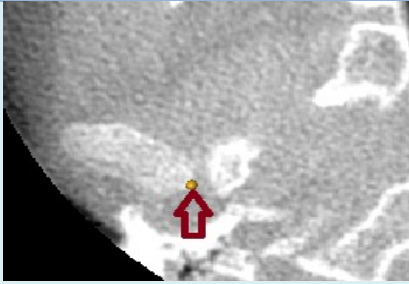
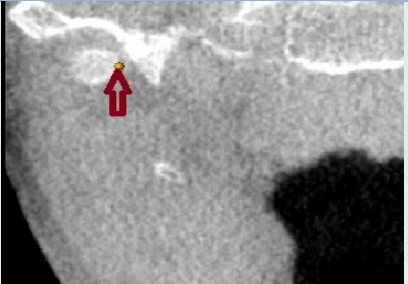
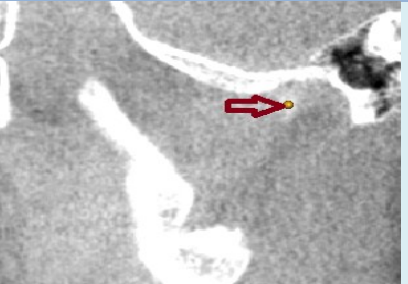
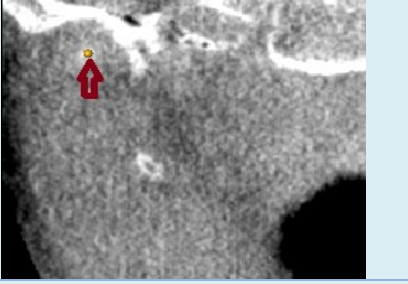
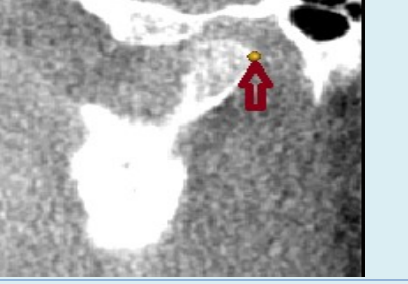
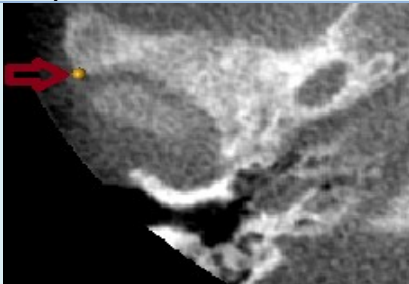
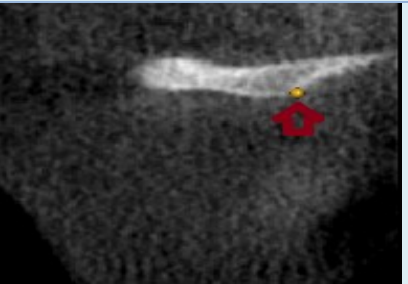
Coronal Plane Reference Landmarks	Right infra- orbital foramen	Left infra- orbital foramen	Nasion	

Table 3.2 Landmarks definitions.

Landmark	Axial plane	Coronal plane	Sagittal plane
Foramen Magnum	Most anterior mid-point of foramen Magnum	Most inferior mid-point of foramen Magnum	Most inferior point of the foramen magnum
CBCT			
Nasion	Most anterior mid-point of the frontonasal suture that joins the nasal part of the frontal bone and the nasal bones on the sagittal and coronal plane	Most anterior point of the frontonasal suture that joins the nasal part of the frontal bone and the nasal bone in the facial midline	Most anterior point of the frontonasal suture that joins the nasal part of the frontal bone and the nasal bones
CBCT			
Mid-point between Infraorbital Foramen	Mid-point between Infraorbital Foramen	Mid-point between Infraorbital Foramen	Mid-point between Infraorbital Foramen
CBCT	A calculated midpoint between 2 Infraorbital Foramen	The calculated midpoint between 2 Infraorbital Foramen	The calculated midpoint between 2 Infraorbital Foramen
Foramen Oval	Center of the smallest inferior circumference	Mid-point between the lateral edges of the sphenoid bone	Mid-point between the anterior and posterior edges of the sphenoid bone

CBCT			
Infra-orbital foramen	on the most anterior point of the infraorbital ridge above infraorbital foramen on birds-eye view 3D (volume rendering isso-surface) view	The point on the infraorbital ridge above midpoint-infraorbital foramen on frontal 3D (volume rendering isso-surface) view	The most anterior surface of the Infraorbital ridge above mid-infraorbital foramen on lateral view 3D (volume rendering isso-surface) view
CBCT			
Lateral Condyle	Most lateral mid-point of the condyle	Most lateral point of the condyle	Center of the most lateral point of the condyle
CBCT			

Medial Condyle	Most medial mid-point of the condyle	Most medial point of the condyle	Center of the most medial point of the condyle
CBCT			
Posterior Condyle	Most posterior point of the medial part of the condyle	Center of the most posterior point of the condyle	Most posterior point of the condyle
CBCT			
Antero-lateral Glenoid Fossa	Antero-lateral point of the fossa. The intersection between the lateral fossa and the zygomatic part of the temporal bone	Most inferolateral part of the fossa	Most inferior point of the anterior slope of the fossa
CBCT			

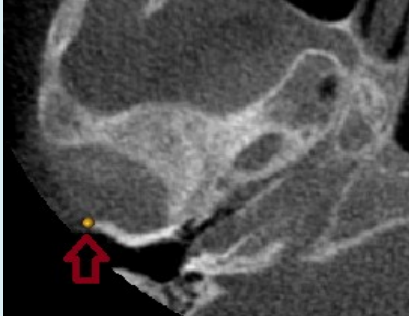
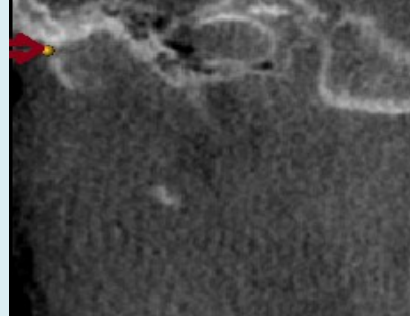
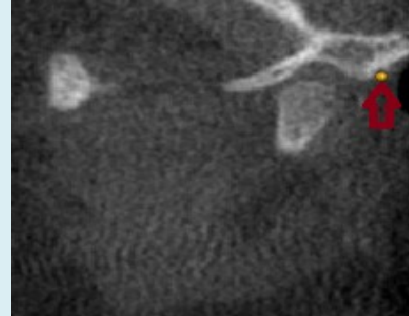
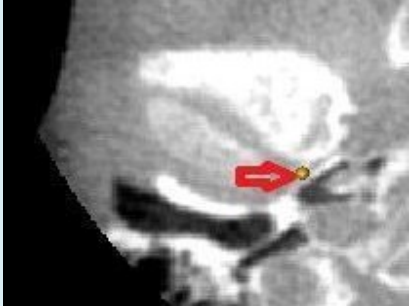
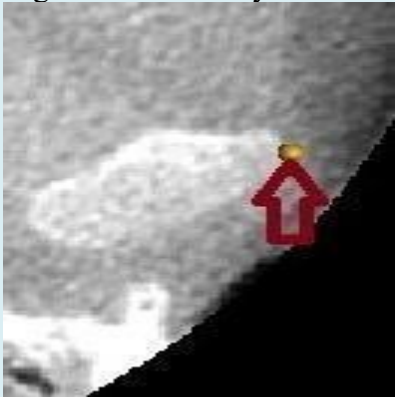
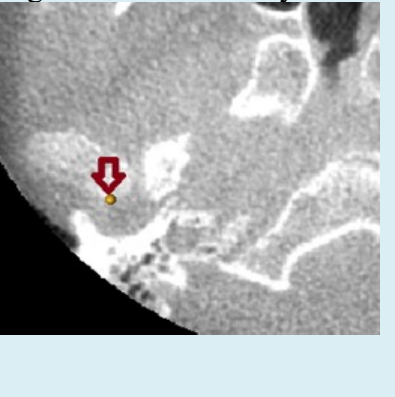
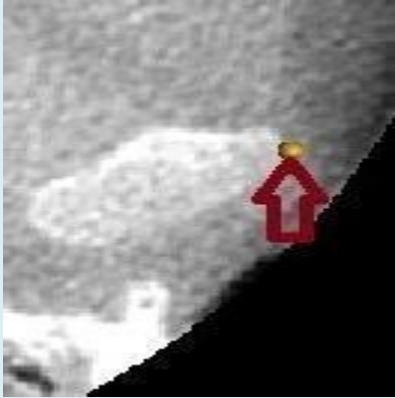
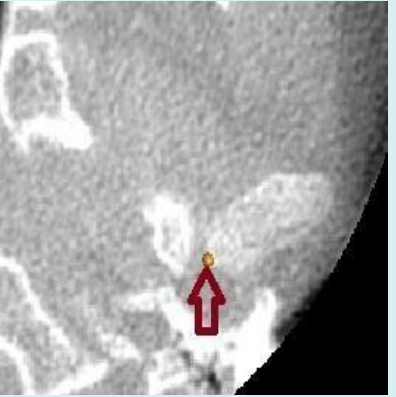
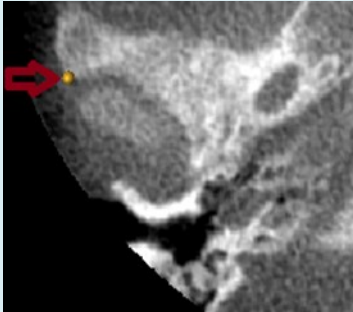
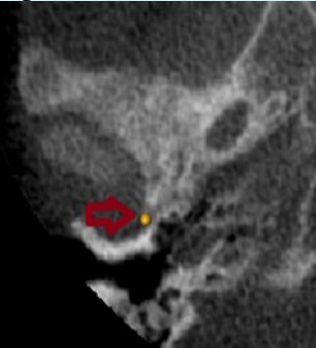
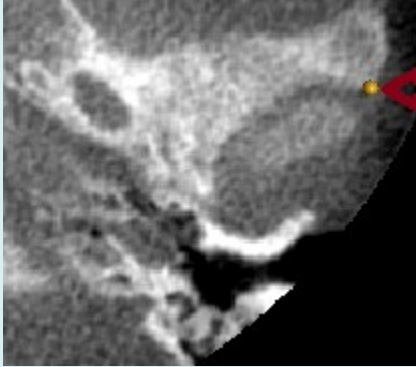
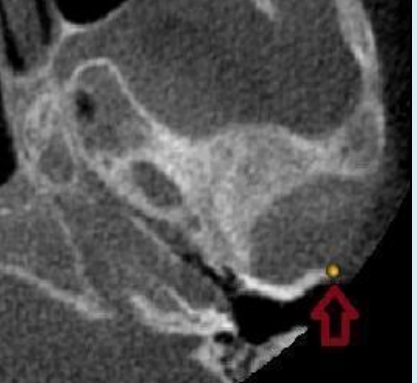
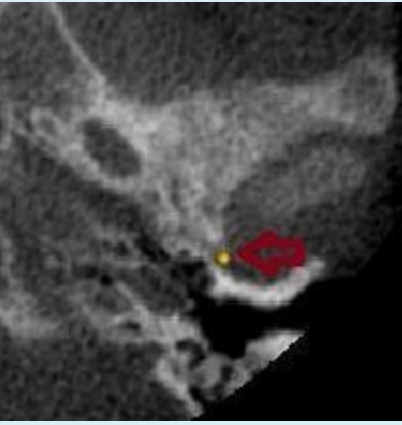
Postero-lateral Glenoid Fossa	Postero-lateral part of the fossa. The intersection between the fossa and the tympanic part of the temporal bone	Depression created between the inferior posterior fossa wall and the superior tympanic part of the temporal bone	Just posterior to the apex of the post-glenoid process
CBCT			
Medial Glenoid Fossa	Postero-medial point of the fossa. Facing the depression of squamous-tympanic suture at the level of the superior part of the vertical portion of the carotid canal	The most medial part of the fossa facing the depression of the squamotypanic suture	Most inferior point of the squamous-tympanic suture between the anterior and posterior edge of the suture
CBCT			

Table 3.3 Landmarks of condyle and fossa.

Landmark category	Landmark 1	Landmark 2	Landmark 3	
Condylar landmark	Right-Lateral Condyle 	Right- Medial Condyle 	Right- Posterior Condyle 	
	Landmark 4	Landmark 5	Landmark 6	
	Left- Lateral Condyle 	Left- Medial Condyle 	Left- Posterior Condyle 	
	Fossa landmarks	Landmark 1	Landmark 2	Landmark 3

<p>Right- Antero-lateral Glenoid Fossa</p> 	<p>Right- Postero-lateral Glenoid Fossa</p> 	<p>Right- Medial Glenoid Fossa</p> 
<p>Landmark 4</p>	<p>Landmark 5</p>	<p>Landmark 6</p>
<p>Left- Antero-lateral Glenoid Fossa</p> 	<p>Left- Postero-lateral Glenoid Fossa</p> 	<p>Left- Medial Glenoid Fossa</p> 

### **3.2.4 The hypothesis of intra-rater reliability**

Preceding any measuring equipment or evaluation tool may be utilized in research or therapeutic settings, proving its reliability is necessary. The term "reliability" refers to the capacity of measurements to be repeated (Koo & Li, 2016). The degree of correlation and agreement between measurements are considered (Portney LG & Watkins MP, 2000). Mathematically, the reliability value spans from 0 to 1, with values nearer to 1 indicating more dependability (Koo & Li, 2016). Historically, dependability was determined using the Pearson correlation coefficient, paired t-test, and Bland-Altman plot. On the other hand, the paired t-test and Bland-Altman plot are techniques for assessing agreement, while the Pearson correlation coefficient is a measure of correlation and is not a preferred test of reliability. A more acceptable measure of dependability would represent the degree of correlation between measurements and the degree of agreement between measurements. Such is provided by the intraclass correlation coefficient (ICC) (Koo & Li, 2016). ICC can evaluate how strongly reliable the landmarks in each group were. Values between 0.75 and 0.9 are regarded as good and above 0.9 as excellent (Koo & Li, 2016).

Intra-rater reliability tests were conducted prior to data collection for the primary research to assess the reliability of the landmark measurements. Additionally, measurement errors can be considered for comparisons of intra-rater reliability.

The reliability analyses include the following hypotheses:

H<sub>0</sub>: The correlation between within-researcher measurements is equal to zero.

H<sub>a</sub>: The correlation between within-researcher measurements is not equal to zero.

### 3.2.5 Intra-rater reliability design

The volumes obtained using the CBCT are true representations of accurate anatomic linear measures (1:1) of three-dimensional anatomic components (Lagravère et al., 2008). The three-dimensional surface accuracy of CBCT scans demonstrates acceptable intra- and inter-assessor reliability when measuring distances on a stiff facial surface (Moerenhout et al., 2009).

Moreover, it has been shown that linear measurements conducted on 3-D surface models are more accurate when compared to anatomical measurements done with a direct calliper (Damstra et al., 2011). CBCT models with voxel sizes ranging from 0.25-0.4 mm showed a mean absolute error of  $0.07 \pm 0.05$  mm to  $0.05 \pm 0.04$  mm. Moreover, CBCT showed excellent levels of agreement and an intra-class correlation coefficient (ICC) of  $> 0.99$ . On the other hand, the measurement errors associated with 3D cephalometric measurements generated by CBCT might be deemed clinically significant. This error raises concerns about using linear and angular 3D measures for detecting actual treatment effects when high accuracy is needed (Damstra et al., 2011).

A total of 19 sets of anatomic landmarks were examined (Table 3.2), comprising three single midline landmarks (including calculated midline between Infraorbital foramina), one pair in the cranial base, one pair in the face, and six pairs related to the TMJ (Table 3.3). These landmarks were identified three times (at least one day apart) for 10 CBCT randomly selected from the complete study set of CBCT images.

All CBCT scans were exported as DICOM files and then imported into the AVIZO LITE© Berlin, Thermo Fisher Science 2019.1 programme for analysis. For each CBCT volume, a Cartesian coordinate system was utilized, with the origin of the X, Y, and Z axes identified during the scan. Three planes were used to visualize the CBCT volumes: the x-y axial (right-left), the x-z coronal (superior-inferior), and the y-z sagittal (anterior-posterior).

The intraclass correlation coefficient (ICC) was used to determine the landmark reliability's tracing location. Between 0.75 to 0.9 is considered good, while more than 0.9 is considered excellent (Koo & Li, 2016). The mean of the deducted differences between each coordinate (X, Y, Z) and the mean of the X, Y, and Z differences values for the three trials were calculated. The term "measurement errors" refers to this. The results are included in the next chapter's appropriate section.

### **3.3 Statistical methods**

#### **3.3.1 General overview**

Version 28 of IBM SPSS© 2021 Statistics 64-bit Window edition was used to conduct the statistical analysis. The MANOVA statistical technique was used to determine significant differences between the three study groups in each dimension (anteroposterior, vertical, and mediolateral) of the condyle and fossa landmarks jointly, the condyle landmarks, and the fossa landmarks. All statistical analyses were conducted with a significance threshold Alpha of 0.05 except for Box's M test, as a p-value of 0.001 was used (Nimon, 2012). Moreover, corrected alpha was implicated when necessary to correct the inflation of alpha.

The following variables are included in this study: types of treatment, which are nominal and have three categories (Xbow, Herbst, and control); gender, which is nominal and has two categories (male and female); age at which treatment started, which is continuous and is expressed in years; the axial, sagittal, and coronal plane distance to the condylar and glenoid fossa landmarks points which is continuous and is expressed in mm; and the total CBCT time between T0 and T1 which was represented as a continuous variable in months. Given that only two-time points were measured in this study (T0 and T1), a spreadsheet was used to calculate the amount of positional change in distance in condylar and glenoid fossa landmarks relative to reconstructed planes (axial, sagittal, and coronal) between the two-timeline points (pre-treatment -T0 and post-treatment -T1).

This study identified 36 dependable variables representing the condylar and glenoid fossa landmarks of all three dimensions. The number of dependent variables of all condylar and fossa landmarks jointly of each dimension is 12 variables. The number of dependent variables of the condylar or fossa landmarks separately for each dimension is six, and one independent variable (treatment type) was used. One-way MANOVA was the test chosen to perform the principal general analysis. Overall, nine one-way MANOVA will be performed.

### **3.3.2 Description of statistical analysis**

A description of the prospective statistical analysis is as follows:

- 1- Descriptive statistics.

- 2- One-way ANOVA: Test the difference in baseline data (age) between the groups and the difference in the time interval duration between T0 and T1.
- 3- Chi-square: Test the baseline (gender) difference between the treatment group.
- 4- Pre-MANOVA assumption tests.
- 5- One-way MANOVA to answer the primary research question. The hypotheses defining the primary research question and objective are:

- Concerning the anteroposterior positional change:

H01.1: When considered jointly, there is no difference in the mean variation distance between the groups of the condylar and glenoid fossa landmarks to the coronal reconstructive plane in the anteroposterior dimension.

Ha1.1: When considered jointly, there is a difference in the mean variation distance between the groups of the condylar and glenoid fossa landmarks to the coronal reconstructive plane in the anteroposterior dimension.

H01.2: When considered jointly, there is no difference in the mean variation distance between the groups of the condylar landmarks to the coronal reconstructive plane in the anteroposterior dimension.

Ha1.2: When considered jointly, there is a difference in the mean variation distance between the groups of the condylar landmarks to the coronal reconstructive plane in the anteroposterior dimension.

H01.3: When considered jointly, there is no difference in the mean variation distance between the groups of the glenoid fossa landmarks to the coronal reconstructive plane in the anteroposterior dimension.

Ha1.3: When considered jointly, there is a difference in the mean variation distance between the groups of the glenoid fossa landmarks to the coronal reconstructive plane in the anteroposterior dimension.

- Concerning the vertical positional change:

H02.1: When considered jointly, there is no difference in the mean variation distance between the groups of the condylar and glenoid fossa landmarks to the axial reconstructive plane in the vertical dimension.

Ha2.1: When considered jointly, there is a difference in the mean variation distance between the groups of the condylar and glenoid fossa landmarks to the axial reconstructive plane in the vertical dimension.

H02.2: When considered jointly, there is no difference in the mean variation distance between the groups of the condylar landmarks to the axial reconstructive plane in the vertical dimension.

Ha2.2: When considered jointly, there is a difference in the mean variation distance between the groups of the condylar landmarks to the axial reconstructive plane in the vertical dimension.

H02.3: When considered jointly, there is no difference in the mean variation distance between the groups of the glenoid fossa landmarks to the axial reconstructive plane in the vertical dimension.

Ha2.3: When considered jointly, there is a difference in the mean variation distance between the groups of the glenoid fossa landmarks to the axial reconstructive plane in the vertical dimension.

- Concerning the mediolateral positional change:

H03.1: When considered jointly, there is no difference in the mean variation distance between the groups of the condylar and glenoid fossa landmarks to the sagittal reconstructive plane in the mediolateral dimension.

Ha3.1: When considered jointly, there is a difference in the mean variation distance between the groups of the condylar and glenoid fossa landmarks to the sagittal reconstructive plane in the mediolateral dimension.

H03.2: When considered jointly, there is no difference in the mean variation distance between the groups of the condylar landmarks to the sagittal reconstructive plane.

Ha3.2: When considered jointly, there is a difference in the mean variation distance between the groups of the condylar landmarks to the sagittal reconstructive plane in the mediolateral dimension.

H03.3: When considered jointly, there is no difference in the mean variation distance between the groups of the glenoid fossa landmarks to the sagittal reconstructive plane in the mediolateral dimension.

Ha3.3: When considered jointly, there is a difference in the mean variation distance between the groups of the glenoid fossa landmarks to the sagittal reconstructive plane in the mediolateral dimension.

6- MANOVA: Answer the secondary research questions if the primary research question was affirmative (statistically and clinically significant).

Ho1: There is no difference in the mean variation in distance from the condylar and glenoid fossa landmarks to the reconstructive planes (coronal, axial, and sagittal) pre-and post-treatment (T0-T1) timeline between the type of treatments.

Ha1: There is a difference in the mean variation in distance from the condylar and glenoid fossa landmarks to the reconstructive planes (coronal, axial, and sagittal) pre-and post-treatment (T0-T1) timeline between the type of the treatment.

Ho2: There is no difference in the mean variation in distance from the condylar and glenoid fossa landmarks to the reconstructive planes (coronal, axial, and sagittal) pre-and post-treatment (T0-T1) timeline between females and males.

Ha2: There is a difference in the mean variation in distance from the condylar and glenoid fossa landmarks to the reconstructive planes (coronal, axial, and sagittal) pre-and post-treatment (T0-T1) timeline between females and males.

Ho3: When considering the timeline duration, there is no difference in the mean variation distance from the condylar and glenoid fossa landmarks to the reconstructive planes (coronal, axial, and sagittal).

Ha3: When considering the timeline duration, there is a difference in the mean variation distance from the condylar and glenoid fossa landmarks to the reconstructive planes (coronal, axial, and sagittal).

Ho4: When considering the age at the start of treatment, there is no difference in the mean variation in distance from the condylar and glenoid fossa landmarks to the reconstructive planes (coronal, axial, and sagittal) pre-and post-treatment (T0-T1) timeline.

Ha4: When considering the age at the start of treatment, there is a difference in the mean variation in distance from the condylar and glenoid fossa landmarks to the reconstructive planes (coronal, axial, and sagittal) pre-and post-treatment (T0-T1) timeline.

### **3.3.3 Ethical approval**

CBCTs and data were gathered from patients who participated in a comprehensive study, “Skeletal, Functional And Dental Changes During Treatment Of Mild to Moderate Class II Malocclusions With Fixed Class II Correctors: A Randomized Clinical Trial” (Study ID of

ethical approval Pro00045191). The University of Alberta's The Health Research Ethics Board re-approved for the project on January 21, 2022.

## **Chapter 4: Results; Intra-rater reliability analyses; Measurements of the landmarks positional change of the TMJ**

### **4.1 Intra-Rater Reliability**

#### **4.1.1 Intra-rater reliability results of landmark points**

Given the large number of tests conducted, the Bonferroni technique was used to alter the p-value of 0.05 to reduce type 1 error, yielding an adjusted p-value of 0.0026 as a consequence (Lee & Lee, 2018). The null hypothesis can be rejected, accepting the alternative hypothesis that the correlation within-researcher measurements are not equal to zero for all traced landmark points -as the p-value was less than 0.0026 for all landmark points. The ICC for all the measures was more than 0.98. As a result, this approach demonstrates excellent reliability under the specified circumstances (Table 4.1) (Koo & Li, 2016). Furthermore, the upper and lower boundaries of the confidence intervals (CIs) of every landmark point traced on CBCT were > 0.90; This was true for both the upper and lower bounds of the CIs of all landmark points traced on CBCT (Table 4.1).

Table 4.1 Intraclass correlation coefficient (95% confidence interval) and p-value. Please notice that the values were rounded to the second decimal except for the p-value.

<b>Landmark</b>	<b>ICC average measure X (lower- upper bound confidence interval)</b>	<b>ICC average measure Y (lower- upper bound confidence interval)</b>	<b>ICC average measure Z (lower-upper bound confidence interval)</b>	<b>P-value of ICC (X; Y; Z)</b>
1- Foramen Magnum (FM)	0.98 (0.96-0.99)	0.99 (0.99-1)	1 (1-1)	<0.0026; <0.0026; <0.0026
2- Right Foramen Oval (RFO)	0.98 (0.94-0.99)	0.99 (0.98-1)	1 (1-1)	<0.0026; <0.0026; <0.0026
3- Left Foramen Oval (LFO)	0.98 (0.96-0.99)	0.99 (0.99-0.99)	1 (1-1)	<0.0026; <0.0026; <0.0026
4- Nasion (N)	0.99 (0.98-0.99)	1 (1-1)	1 (0.99-1)	<0.0026; <0.0026; <0.0026
5- Midpoint between the two-Infraorbital Foramen (MIOF)	1 (0.99-1)	1 (1-1)	1 (1-1)	<0.0026; <0.0026; <0.0026
6- Right Infraorbital Foramen (RIO)	1 (1-1)	1 (1-1)	1 (1-1)	<0.0026; <0.0026; <0.0026
7- Left Infraorbital Foramen (LIO)	1 (0.99-1)	1 (1-1)	1 (1-1)	<0.0026; <0.0026; <0.0026
8- Right Lateral Condyle (RLC)	1 (1-1)	1 (0.99-1)	1 (1-1)	<0.0026; <0.0026; <0.0026
9- Right Medial Condyle (RMC)	1 (1-1)	1 (1-1)	1 (1-1)	<0.0026; <0.0026; <0.0026
10- Right Posterior Condyle (RPC)	1 (0.99-1)	1 (1-1)	1 (1-1)	<0.0026; <0.0026; <0.0026
11- Right Antero-lateral Glenoid Fossa (RALGF)	1 (0.99-1)	1 (0.99-1)	1 (1-1)	<0.0026; <0.0026; <0.0026

12- Right Postero-lateral Glenoid Fossa (RPLGF)	1 (0.99-1)	1 (1-1)	1 (1-1)	<0.0026; <0.0026; <0.0026
13- Right Medial Glenoid Fossa (RMGF)	1 (0.99-1)	1 (1-1)	1 (1-1)	<0.0026; <0.0026; <0.0026
14- Left Lateral Condyle (LLC)	1 (1-1)	1 (1-1)	1 (1-1)	<0.0026; <0.0026; <0.0026
15- Left Medial Condyle (LMC)	1 (1-1)	1 (1-1)	1 (1-1)	<0.0026; <0.0026; <0.0026
16- Left Posterior Condyle (LPC)	1 (0.99-1)	1 (1-1)	1 (1-1)	<0.0026; <0.0026; <0.0026
17- Left Antero-lateral Glenoid Fossa (LALGF)	0.99 (0.98-1)	1 (1-1)	1 (1-1)	<0.0026; <0.0026; <0.0026
18- Left Postero-lateral Glenoid Fossa (LPLGF)	1 (0.99-1)	1 (1-1)	1 (1-1)	<0.0026; <0.0026; <0.0026
19- Left Medial Glenoid Fossa (LMGF)	0.99 (0.97-1)	1 (1-1)	1 (1-1)	<0.0026; <0.0026; <0.0026

Analysis of the related measurement error for each landmark on each axis confirmed the reliability shown by the ICC values, with a measurement error of less than 1 mm for all landmarks on all axes (Appendix, Table A3.2).

#### **4.1.2 Intra-rater reliability results in the distance from each reconstructive plane to the condylar and glenoid fossa landmarks**

The entire protocol and methodology to calculate the distance from each reconstructive plane and reconstruction of each plane are explained in Chapter 3 (Generation of the planes and measurement of the perpendicular distance).

The mean distance difference for the repeated measurement for each CBCT from each condylar and glenoid fossa landmark to each reference plane was calculated. The measurement error showed a higher value than the landmark point measurement error. Descriptive data with comments are illustrated in Appendix (Table A3.1).

The mean distance difference for the repeated measurement between landmarks within each TMJ was calculated. The measurement error ranged from 0.4-0.5 mm, suggesting minimal measurement error because it is less than the radiological significance (0.6 mm) (Table 4.2).

Table 4.2 Measurement error for distance measurements within the TMJ (intra-joint distance in mm); and standard deviation (SD). Please notice that the values were rounded to the first decimal place in mm.

Distance between landmarks (Landmark 1: Landmark 2)	Mean in mm (SD)
Right Lateral Condyle: Right Antero-lateral Glenoid Fossa	0.4 (0.2)
Right Medial Condyle: Right Medial Glenoid Fossa	0.5 (0.3)
Right Posterior Condyle: Right Postero-lateral Glenoid Fossa	0.5 (0.3)
Left Lateral Condyle: Left Antero-lateral Glenoid Fossa	0.5 (0.3)
Left Medial Condyle: Left Medial Glenoid Fossa	0.5 (0.3)
Left Posterior Condyle: Left Postero-lateral Glenoid Fossa	0.5 (0.3)

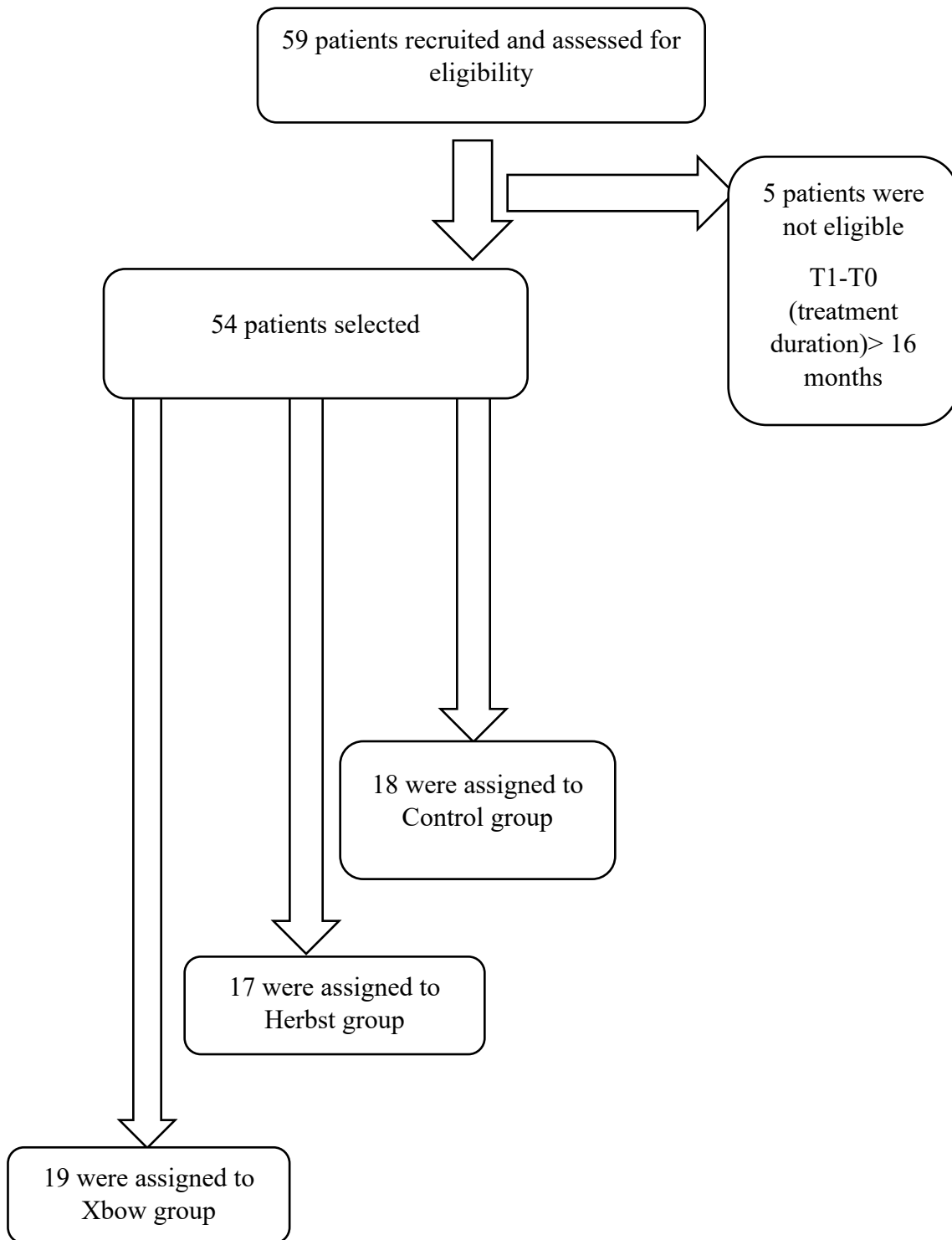
## 4.2 Results of the research

### 4.2.1 Losses and exclusions

The original sample included in the study was 59 subjects. Five were subsequently excluded because the time interval between T0 and T1 CBCT images was more than 16 months, resulting in a final sample size of 54 subjects.

- 18 were assigned to the Control group (watchful waiting)
- 17 were assigned to the Herbst group
- 19 were assigned to the Xbow group

#### 4.2.2 Participant flow



A one-way ANOVA test can observe any differences between the groups regarding age at the start of the treatment. The resulting p-value was  $>0.05$ , indicating no statistically significant differences between the three groups (Herbst, Xbow, and control) (Table 4.4). Because gender is a dichotomous variable, the Chi-Square test was used to compare the three proportions, and the results indicated no significant difference in sex between the three groups ( $p > 0.05$ ). (Table 4.4).

One-way ANOVA was used to test the difference in the mean duration of treatment between the three groups. The duration of treatment was defined as T1 minus T0 in months. Again, the resulting p-value was  $>0.05$ , indicating no statistically significant differences in the mean duration of treatment (T1-T0) between the three groups of the study (Table 4.3).

Table 4.3 Descriptive analysis of age (years) and time interval duration (months).

Variable	Control	Herbst	Xbow	Total
Age in years: Mean (Standard deviation)	12.6 (1.1)	12.9 (1.1)	12.3 (1.2)	12.6 (1.2)
The duration between T0 and T1 in months: Mean (Standard deviation)	12.2 (0.7)	12.7 (1.2)	12.4 (1)	12.4 (1)

Table 4.4 Gender distribution among groups.

Group	Female	Male	Total cases (%)
Control: Cases (%)	8 (44%)	10 (56%)	18 (33%)
Herbst: Cases (%)	9 (53%)	8 (47%)	17 (31%)
Xbow: Cases (%)	7 (37%)	12 (63%)	19 (35%)

### 4.2.3 Pre-MANOVA assumption tests

Checking to verify that the following assumptions are satisfied whenever MANOVA is performed is recommended:

- 1- Independence: each observation is chosen from the population without regard to the others. This assumption was satisfied since the patients in the study were selected, so that acquisition of the CBCT from one patient does not affect the acquisition of the CBCT from other patients.
- 2- Dependent variables are ratio, intervals, or continuous: as preset in this trial, our dependent variables are continuous variations in orthogonal distances, which fulfil this assumption.
- 3- Variants are normally distributed: this means that response variables are normally distributed within each group of the factor variable. Shapiro-Wilk normality test was performed for each variable of each orthogonal variation to each plane (coronal, axial,

and sagittal) within each treatment group (control, Herbst, and Xbow) of all 12 landmarks. The Shapiro-Wilk test was p-value was  $>0.05$  for each variable of each orthogonal variation distance to each plane (coronal, axial, and sagittal) within each treatment group (control, Herbst, and Xbow) of all 12 landmarks. Thus, concluding that the variables are normally distributed within the groups.

- 4- Absence of extreme outliers: Boxplots (Appendix, Figure A3.1) was performed and showed each variable corresponding to each orthogonal variation to each plane (coronal, axial, and sagittal) within each treatment group (control, Herbst, and Xbow) of all 12 landmarks. No potential outliers were detected, which fulfills this assumption.
- 5- Adequate sample size: it is advised that the number of cases in each group is more than the number of dependent variables analyzed using MANOVA. In this research, the maximum dependent variable/MANOVA test is 12 dependable variables, and the least number of cases per group is 17 cases, which fulfills this assumption.
- 6- Equality of variance-covariance matrices: the population variance-covariance matrix is recommended to be homogeneous. In order to compare covariance in multivariate data, Box's M test was utilized. A note worth mentioning for this test is that, generally, a significant alpha level of  $<0.001$  is usually used in most cases for Box's M test (Nimon, 2012). Box's M test p-value was  $> 0.001$ , failing to reject the null hypothesis (covariances matrices are equal across the groups) and fulfill the equality assumption.

7- Linearity: means that each pair of dependent variables for each independent variable group has a linear relationship with the independent variable. Scatterplot matrices (Appendix, Figure A3.2) were performed and showed each paired variable corresponding to each orthogonal variation to each plane (coronal, axial, and sagittal) within each treatment group (control, Herbst, and Xbow). Visual evaluation of the linearity of all pairs of response variables (Appendix; Figure A3.2) showed that not all the cells exhibit the conventional linear or elliptical pattern. However, one could report Pillai's Criterion instead of Wilk's Lambda. Pillai's trace is robust to violations of assumptions (Barbara G. Tabachnick & Linda S. Fidell, 2007; James H. Bray & Scott E. Maxwell, 1985), especially when there is an equal or nearly equal sample between the groups, which is the case in this research. Wilks' lambda is the most commonly used method, and it evaluates whether the data under the assumption of an equal population mean vector for all groups are more likely than the data under the assumption that population mean vectors are similar to those of the sample mean vectors for each group. On the other hand, Pillai's criteria use the aggregated effect variances (Barbara G. Tabachnick & Linda S. Fidell, 2007). Regarding the MANOVA test, Pillai's Criterion will be reported in this research.

#### **4.2.4 One-way MANOVA test for all landmarks jointly, condylar landmarks, and fossa landmarks corresponding to each dimension (anteroposterior, vertical and mediolateral)**

Matrices expressing thesis hypotheses are illustrated in Appendix (Figure A3.3). Furthermore, the mean positional change for each landmark (36 variables) regarding each dimension is illustrated in Appendix (Table A3.3).

One-way MANOVA was conducted nine times to determine whether there was a mean difference between the groups. The test was performed three times, corresponding to each dimension (anteroposterior, vertical, and mediolateral positional change). Moreover, within each dimension, means of variations in the orthogonal distance between T1-T0 were tested for the condyle and glenoid fossa landmarks jointly, condylar landmarks, and the fossa landmarks (Table 3.5).

Regarding the anteroposterior positional change, there was a non-significant difference in means of variations in the orthogonal distance of the condyle and glenoid fossa landmarks jointly based on the comparison groups (Herbst, Xbow, and Control),  $F(24, 82) = 0.78$ ,  $p > 0.05$ ; Pillai's trace = 0.37. Moreover, there was a non-significant difference in means of variations in the orthogonal distance of the condylar landmarks jointly based on the comparison groups,  $F(12, 94) = 1.28$ ,  $p > 0.05$ ; Pillai's trace = 0.28, and there was a non-significant difference in means of variations in the orthogonal distance of the glenoid fossa landmarks jointly based on comparison groups,  $F(12, 94) = 0.57$ ,  $p > 0.05$ ; Pillai's trace = 0.14.

Regarding the vertical positional change, there was a non-significant difference in means of variations in the orthogonal distance of the condyle and glenoid fossa landmarks jointly based on the comparison groups (Herbst, Xbow, and Control),  $F(24, 82) = 1.51$ ,  $p > 0.05$ ; Pillai's trace = 0.61. Moreover, there was a non-significant difference in means of variations in the orthogonal distance of the condylar landmarks jointly based on the comparison groups,  $F(12, 94) = 1.79$ ,  $p$

$> 0.05$ ; Pillai's trace = 0.37, and there was a non-significant difference in means of variations in the orthogonal distance of the glenoid fossa landmarks jointly based on the comparison groups,  $F(12, 94) = 1.71, p > 0.05$ ; Pillai's trace = 0.36.

Regarding the mediolateral positional change, there was a non-significant difference in means of variations in the orthogonal distance of the condyle and glenoid fossa landmarks jointly based on the comparison groups (Herbst, Xbow, and Control),  $F(24, 82) = 0.79, p > 0.05$ ; Pillai's trace = 0.37. Moreover, there was a non-significant difference in means of variations in the orthogonal distance of the condylar landmarks jointly based on the comparison groups,  $F(12, 94) = 0.79, p > 0.05$ ; Pillai's trace = 0.18, and there was a non-significant difference in means of variations in the orthogonal distance of the glenoid fossa landmarks jointly based on the comparison groups,  $F(12, 94) = 1.08, p > 0.05$ ; Pillai's trace = 0.24.

Concerning all of the one-way MANOVA tests, failing to reject the null hypothesis and conclude that there is no difference between the comparison groups (Herbst, Xbow, and control) means variations in the orthogonal distance between the T1-T0 timeline in all dimensions when the measures are considered for the landmarks of the condyle and glenoid fossa jointly, condyle separately, or glenoid fossa separately. There are no further statistical tests required or conducted (Table 4.5).

Table 4.5 Summary of nine MANOVA tests of multiple landmark settings means variation in positional change corresponding to each plane. Notice that the values were rounded to the second decimal place.

Landmark tested	Relative plane	Pillai's value	F	Hypothesis df	Error df	p-value
Anteroposterior positional change						
Condyle and glenoid fossa	Coronal	0.37	0.78	24	82	>0.05
Condylar	Coronal	0.28	1.28	12	94	>0.05
Glenoid fossa	Coronal	0.14	0.57	12	94	>0.05
Vertical positional change						
Condyle and glenoid fossa	Axial	0.61	1.51	24	82	>0.05
Condylar	Axial	0.37	1.79	12	94	>0.05
Glenoid fossa	Axial	0.36	1.71	12	94	>0.05
Mediolateral positional change						
Condyle and glenoid fossa	Sagittal	0.37	0.79	24	82	>0.05
Condylar	Sagittal	0.18	0.79	12	94	>0.05
Glenoid fossa	Sagittal	0.24	1.08	12	94	>0.05

## **Chapter 5: Discussion and conclusions**

### **5.1 Discussion of the study**

#### **5.1.1 Discussion of previous research limitations and methods implied in this thesis to overcome the previous limitations**

The previous research limitations fall into five categories: failure to compare class II correctors (Herbst and Xbow) in one sitting, failure to include a control group, using a 2-dimensional evaluation module, failure to investigate the TMJ (condyle and fossa), and design-related limitations.

In contrast to some studies, our research explores the effect of Herbst and Xbow appliances in one setting. This methodology allows the comparison of different mechanisms of action between the Herbst and Xbow appliances. As the mechanism differs, then the effect can be different. Some prior literature has explored the effects of the Xbow and Herbst appliances individually and compared them to other orthopedic appliances (Flores-Mir et al., 2009; Pancherz, 1979; Pancherz et al., 1999; Randeep S. Chana, 2013; Souki et al., 2017), but they have not looked into the effects of the Herbst and Xbow appliances in combination. As a result, there has been no direct comparison between the variations in the treatment of these two fixed functional appliances (Herbst and Xbow) in these researches.

Including a control group is crucial, as it can be used for comparison benefits from approximating what would have occurred in the treated patients if no therapy had been administered. Consequently, the actual effect (in this example, the usage of the Herbst and Xbow appliances) can be evaluated and distinguished from the positional changes anticipated due to growth. Therefore, it was preferable to have a control group whose development potential was comparable to the two experimental groups. We included a control group that featured a class II malocclusion as the other treatment groups in the current study. Moreover, the growth potential without treatment was standardized in this control group, with similar non-significant baseline characteristics and CBCT acquisition timeline ( $p>0.05$ ). Moreover, our control group was not a historical record (Papageorgiou et al., 2017) with unreliable clinical features but rather a designed group meant for comparison.

Our research uses a CBCT image modality for evaluation; a CBCT provides 3-dimensional data in all planes (anteroposterior, vertical, and mediolateral) compared to other 2-dimensional imaging. Some research examining Herbst's and Xbows employed two-dimensional cephalogram imaging techniques (Baltromejus S et al., 2002; Flores-Mir et al., 2009). Moreover, the 2-dimensional imaging technique may not adequately depict the complex structures and three-dimensional changes throughout treatment (Durão et al., 2013). Aside from that, errors in cephalograms like magnification errors and poor landmark repeatability are vital difficulties that might undermine the trustworthiness of such investigations (Durão et al., 2013). For example, compared to conventional 2-dimensional radiographs, CBCT provide more informative imaging with minimal or no magnification (Lagravère et al., 2008; Pauwels et al., 2015). CBCTs offer the best 3-dimensional imaging available for hard tissue (Durão et al., 2013).

As a result of completing functional mandibular therapy, a significant emphasis of this thesis is to determine whether or not the condyles and fossae alter their positions, which is a clinical concern in fixed class II corrector treatment (Herbst and Xbow). Although some investigators provided a comparison analysis between the treatment groups (Herbst and Xbow) and included a control group, they did not investigate the TMJ (condyle and fossa) positional change (Insabralde et al., 2021).

Some data from controlled clinical research on humans suggests that functional appliance therapy is related to positional and skeletal changes of the TMJ in the short term compared to controls who did not use a functional appliance. However, the clinical significance and accuracy of these changes remain unclear due to the poor quality of the current data and improper methodological flaws that have been conducted so far. One major drawback of previous studies is evaluating positional change for a limited period of 6 and 9 months (Kyburz et al., 2019). This limitation might influence the magnitude of positional change and does not provide an evaluation of the long-term effect of the appliance, which is more important clinically. Furthermore, the practical use of comparable appliances typically needs 8 to 12 months, at which time the necessary correction should have been achieved (Proffit W et al., 2012). In our research, the time interval between T0 and T1 ranged from 9.6 to 15.6 months (mean=12.4 months). Thus, the actual magnitude of positional change and longer term practical clinical effect of the appliance can be evaluated. Another issue regarding the period between T0 and T1 is the consistency and the difference between the comparison groups. If the treatment groups have a significant

difference in the duration of treatment, the results might show variation in the positional change due to variation in magnitude of growth, not the effect of treatment. We excluded five cases from our sample because they exceeded the duration limit threshold (4 months). Statistically, as a general rule of thumb, any Z-score  $>3$  or  $<-3$  would be considered a true outlier. We calculated the upper (about  $>16$  months) and lower duration threshold (about  $<8$  months) by using the mean duration (12.4 months) and standard deviation (1 month).

In a systematic review, Al-Saleh et al. were unable to establish concrete evidence of the TMJ reaction to the forces applied by the mandibular anterior positioning appliance because of critical design flaws and analytical flaws that prevented them from drawing any definitive conclusions from the literature about the treatments they conducted (Al-Saleh et al., 2015). They recommended that future studies could include the followings to overcome the limitations of previous studies: including an untreated control group, a large sample size with high power, using 3-dimensional CBCT images with pre and post-treatment evaluation, double-blinding of the study, and considering the age and gender difference effect. We included an untreated control group (watchful waiting) with no direct therapeutic action on the condyle and fossa. Moreover, our sample size calculation was based on the estimation of high power (95%). Although our research was not a double-blinded investigation, it was carried out using a single-blinded data evaluator. CBCTs of the patients were numbered, and the patients' data were only exposed when required to be ready to proceed with data gathering. The primary researcher could not discern between T0 and T1 CBCT images visually. However, because the recommended treatment is visually distinct, it was difficult to blind participants or clinicians. This single blinding might partially address blinding drawbacks found in previous studies. Moreover, the author of this

thesis randomized the CBCT files through Microsoft Excel© by randomly rearranging the codes throughout the sheet and tracing each case in order. Finally, the baseline data (age and gender) differences across the groups were not significant ( $p>0.05$ ), which further standardized the sample regarding the baseline data.

### **5.1.2 Operator reliability and error**

Regarding the landmarks reliability in our research, to this date, no exact similar methodologies have been identified in the literature. Consequently, a direct result comparison could not be made. However, other studies have published ICC values that used CBCT measurements of different landmarks. In a recent study, Cheib Vilefort et al. reported an ICCs  $>0.81$  for intra-rater reliability with measurement errors ranging between 0.45 and 0.77 mm (Cheib Vilefort et al., 2019). The ICC in our study (Master thesis) for all the measures was  $> 0.98$ . As a result, this approach demonstrates excellent reliability (Koo & Li, 2016). Our measurement error ranged from 0.1 to 0.9 mm (see Appendix, Table A3.2). Cheib Vilefort et al. used a point-to-point measurement, in contrast to the point-to-plane used in this thesis. The advantage of point-to-point measurement is that it provides an easy, direct method of evaluation and less time to perform the analysis. The calculation of orthogonal distances from a point to a plane is time-consuming, requires more landmarks, and requires a complex calculation through software (in our case Microsoft Excel©). However, the reported reliability for point-to-plane measurement was validated and was more accurate than direct point-to-point measurement (Connie P. Ling, 2016). This conclusion might be because the measurement error is divided across three points distance from each other. Furthermore, according to Liberton and coworkers, the reliability of

the landmarks to each axis on CBCT can be classified according to the standard deviation of variable points to reference points into highly reliable coordinates (standard deviation <1mm, ), reliable (standard deviation between 1 and 2 mm), and unreliable (standard deviation >2mm) (Liberton et al., 2019). Concerning the current thesis, all landmarks' points had a measurement error of less than 1 mm with a maximum standard deviation of 0.6 mm (see Appendix, Table A3.2).

### **5.1.3 Condyle and fossa positional change**

It is essential to know if the condyles reestablish their centric locations inside the glenoid fossa by completing functional mandibular therapy, which is a clinical concern in fixed class II corrector treatment. The use of functional appliances may result in a change in the morphology of the TMJ, which may be caused by a remodelling process of the glenoid fossa and the condyle, which may impact the location of both the condyle and the TMJ disc (Voudouris et al., 2003). It is essential to emphasize that direct comparison between our results and the previous literature was relatively challenging because the methods implied in our research are different from the methods implied in the previous studies (see discussion of previous research limitations in the current chapter). However, an indirect comparison of the results and method implied was viable.

Our results demonstrate that when the Herbst group was compared to the Xbow and control groups, there was no statistically significant ( $p>0.05$ ) mean difference in the position of the glenoid fossa in all dimensions. Thus, consistent with others (Atresh et al., 2018; Katsavrias,

2003; Katsavrias & Voudouris, 2004), any change in the fossa location is of little clinical consequence. In contrast, Rabie et al reported that the suggested skeletal changes generated by the appliance is the anterior displacement of the glenoid fossa, which is supposed to increase the horizontal projection of the mandible (Rabie et al., 2001). The suggested hypothesis is that patients who wear functional appliances have their mandibles moved to a protrusive posture causing their condyles to protrude out of the glenoid fossa, assisting in the correction of Class II. This might promote the development or remodelling of the glenoid fossa into a new location and modify the condyle's position (Pancherz, 1979). An explanation of these inconsistencies might be that these devices are used during the mandible's growth spurt and active growth. Thus, misinterpretation of positional change during expedited growth with a minimal margin of error is expected, especially when the comparison is made without a control group. Also, it might be due to differences in growth because of the different genetic pools as the groups might differ in the severity and class of malocclusion (Proffit et al., 1998) and thus for the treatment. Moreover, a critique of previous studies is that it was mainly animal-based studies or hampered by using two-dimensional and less accurate imaging modalities in their investigations (Rabie et al., 2001; Ruf & Pancherz, 1998). Though the practical use of such appliances typically needs 8 to 12 months, as the necessary correction needs to be achieved (Proffit W et al., 2012), the anterior displacement of the glenoid fossa has been suggested to be only transient (Pancherz & Michailidou, 2004). In our research, the time interval between T0 and T1 ranged from 9.6 to 15.6 months (mean=12.4 months). Thus, the actual magnitude of positional change and a longer clinical effect of the appliance can be evaluated, in comparison to others (Kyburz et al., 2019). In contrast to earlier research, our study has a larger sample size and more reliable 3-dimensional imaging (LeCornu et al., 2013; Rabie et al., 2001; Ruf & Pancherz, 1998).

When the Herbst group was compared to the Xbow and control groups, our results showed a non-statistically significant ( $p>0.05$ ) mean difference in the condyle position in all dimensions. This finding is consistent with Atresh and colleagues, who examined the 3-dimensional locations of the geometric center of the condyle following the Herbst appliance, and reported that there was no statistically significant difference (Atresh et al., 2018). In the context of the condylar and fossa positions jointly or separately, a comparison between the three treatments (control, Herbst, and Xbow) revealed that there was no statistically significant difference in all dimensions ( $p>0.05$ ), regardless of the group used. Thus, it suggests that the Herbst appliance preserves the condyle-glenoid fossa relationship, consistent with earlier research (Atresh et al., 2018; Ruf & Pancherz, 1998). Occlusal correction of the Class II relationship cannot be explained by altered condyle-glenoid fossa relationship. (G. S. M. Kinzinger et al., 2006).

If Herbst's growth modification is valid, then this should accelerate growth. Thus, the protruded mandible will develop quicker, and a more prominent mandible would occur in the presence of therapy. Insabralde et al. using cephalograms, reported statistically significant increased mandibular size among the Herbst group by comparing the mean distance change from condyion to pogonion (Insabralde et al., 2021). Lecornu et al. suggested that anterior mandibular advancement with the Herbst appliance may be attributed to controlling mandibular development, growth direction changes or condylar/fossa position alteration (LeCornu et al., 2013). However, our results do not support condylar/fossa position alteration. The increased mandibular size can be explained by skeletal changes in sites other than the condyle or glenoid

fossa. A postulation to explain this interpretation is that the patient has their mandibles moved to a constant protrusive posture causing their condyles to protrude out of the glenoid fossa when the Herbst appliance is used. Thus, a constant tension effect is produced on the mandible, which might be caused by two points: the anchorage of the appliance to teeth and the anchorage of living structures attaching the condyle to the temporal bone (distraction-like concept). Moreover, the points of primary anchorage represent resistant regions; thus, remodelling in the area of condyle/fossa would not be anticipated in the Herbst appliance, while other regions between these anchorages might represent susceptible regions. This postulation can be supported by our results combined with reports of increased mandibular size among the Herbst group (Insabralde et al., 2021) and by Manfredi et al. investigation, who evaluated the skeletal change of Herbst appliance. They found that only the ramus height and mandibular basal length were significant in males and the mandibular ramus height was significant in females when the total variance was examined (Manfredi et al., 2001).

As the Xbow appliance does not maintain the mandibular protrusion compared to the Herbst appliance, the suggested proposal of skeletal changes generated by the protrusive appliance posture causes the condyles to protrude out of the glenoid fossa might not be favourable to the Xbow appliance (Flores-Mir et al., 2009). Insabralde et al. compared the dental and skeletal effects between Herbst and Xbow appliances. They suggested that Xbow appliances improved the Class II occlusal relation due to primarily dental modifications (Insabralde et al., 2021). This finding was consistent with our results that did not show a significant difference in the position of the condyle and glenoid fossa landmarks in all dimensions of the Xbow group compared to Herbst and controls ( $p > 0.05$ ). Also, our postulation can explain this, as the low forces produced

by the Forsus springs (reportedly about 200 g; (Flores-Mir et al., 2009)) and the patient's ability to sit back the condyle in contrast to the Herbst appliance, as without constant tension produced on the mandible, initiation of expedited skeletal change could not occur.

A point of interest is the volume change in the condyle and fossa of the TMJ following class II fixed functional appliances (Herbst and Xbow). If expedited remodelling of the condyle or fossa is valid following an appliance, then the volume and ratio (condyle to fossa volume ratio) change compared to controls would support the claim that expedited remodelling of the TMJ is valid. There has been no investigation of condyle volume changes after using the Herbst and Xbow appliances compared to controls in terms of the relative change in condyle to fossa volume ratio. However, a recent Master thesis evaluated the mandibular condylar volume and shape changes after using Herbst and the Xbow appliance (al Riyami I, 2021). Worth to mention that they did include a control group for comparison. According to Al Riyami's research findings, all groups showed equal and statistically non-significant differences in condylar volume. There were no distinct patterns of condylar shape alterations, indicating that any changes seen in condyle volume and form may result from normal condylar development. However, they did not investigate the volume ratio change between the condyle and fossa across the different groups, nor did they examine the fossa volume.

#### **5.1.4 Clinical significance of our results**

The current research results showed that the condyle and the glenoid fossa position after therapy with a time interval between T0 and T1 ranging from 9.6 to 15.6 months (mean=12.4 months) did not show a statistically significant difference independent of the type of treatment used (control, Herbst, or Xbow) in all dimensions. Thus, our research might not support the concern that the condyles will be moved into an unphysiological position relative to the fossa using fixed class II correctors (Herbst or Xbow).

#### **5.2 Future recommendations**

- We would recommend a future evaluation of the change in the condyle and glenoid fossa volume and ratio in growing patients following the fixed functional appliance (Herbst, Xbow) compared to controls utilizing CBCT. This suggestion would be advised because of importance of evaluating the volume change in the fossa, and condyle to fossa volume ratio, following class II fixed functional appliances (Herbst and Xbow) to validate the expedited remodelling of the condyle, fossa, and relationship following an appliance.
- Evaluation of the disc of the TMJ three-dimensional positional change using different Class II mandibular positioners/appliances (Herbst, Xbow, and control) utilizing MRI would be advised as the soft tissue contrast and high resolution provided by MRI is critical to accurately assessing the disc location relative to the the condyle and glenoid fossa.

- The postulation that constant tension produced on the mandible can produce a distraction-like effect on different parts of the mandible (other than TMJ) was not investigated. Evaluation of the positional changes of the neck, ramus, and body of the mandible relative to the glenoid fossa following the fixed functional appliance (Herbst, Xbow) and compared to a control group as the skeletal change might occur in another anatomical site such as the neck and ramus of the mandible would be of a great value in supporting or undermining this theory.
- The growth - normal craniofacial development and maturation- would represent a challenge even if we tried every effort to standardize it in this research. Other factors, such as genetic variation that are not reported, can play a role. Although, in this case, the growth modification is not assessed when including an adult sample. However, absolving this factor might provide a better answer to positional change of the condyle regardless of growth. Thus, a future evaluation of positional change of the condyle and glenoid fossa in fully grown adults following mandibular reposition appliances (Herbst and Herbst-like appliance for obstructive sleep apnea) to absolve the growth effect can be of importance.

## 5.3 Limitations

### 5.3.1 Machine limitations

In our research, a voxel size of 0.3 mm was used. When using the voxel size of 0.3mm, the definition of the image obtained by the CBCT may not be sufficient or precise enough to identify minor amounts of the positional shift in the landmarks. This limitation was further exaggerated by using two points (a landmark point and a point present in the reconstructive reference plane) with a total of 0.6 mm anticipated error. As a result, any positional change less than 0.6 mm could not be interpreted as an actual change. However, smaller voxels, which would yield better resolution and more detailed findings, are associated with more extended scanning periods and higher radiation exposure. Furthermore, the notion of ALARA "As Low As Reasonably Achievable " in dental radiography, as proposed by the Centers for Disease Control and Prevention (CDC), should be kept in mind. When the CBCT is employed in conjunction with the voxel size used in this study, the definition of the images created by the CBCT may not be accurate or precise enough to identify small positional changes. However, tiny quantities of positional change that are not recorded are unlikely to be clinically significant.

Other inherent limitations can increase the interpretation error, such as the partial-volume effect (Baumgaertel et al., 2009), beam hardening, and image noise (Pauwels et al., 2015). Moreover, image artifacts (Pauwels et al., 2015) are often seen in dental CBCT images as metal artifacts caused by high levels of X-ray absorption by items with high densities in the imaging field.

However, in this study, landmarks were strategically placed away from potential metal materials, such as amalgam restorations.

The movement of the patient is another cause of tracing inaccuracy. Depending on the amount of motion during the image collecting process. A slight degree of blurring or severe artifacts may appear on the landmark because the relatively lengthy scan periods in CBCT motion might add to tracing error (Pauwels et al., 2015). However, during tracing, there was no evidence of significant movement in our research images. Patients positioned with the inability to lightly touch their teeth in maximum intercuspation during image acquisition with the adolescent population might be another source of measurement inaccuracy. However, this might be a concern in younger children.

### **5.3.2 Avizo© limitations**

The Avizo© program employed in this research has a substantial learning curve that must be overcome, and the investigator in this research had varying degrees of familiarity with the program. Furthermore, the program does not enable simultaneously observing the landmarks in all three planes. The observer must switch planes to verify the landmark's location in various planes. A more user-friendly program might help investigators learn more quickly and efficiently.

The threshold used for iso-surface ranged from 100-400 with a shaded draw style. This technique was implied to incorporate bone window without soft tissue inclusion. Although some soft tissue might incorporate into the iso-surface and the landmark definition accuracy might be affected.

However, because this technique was solely used for one landmark (infra-orbital foramen bilaterally) not the whole plane reconstruction points, the expected effect on the plane displacement might not be great because the landmarks are spread away from each others.

#### **5.4 Conclusions**

When Class II mandibular positioners/appliances (Herbst and Xbow) were compared to the control group, the mean positional changes (anteroposterior, vertical and mediolateral) were not statistically significant regarding the condyle and fossa jointly, condyle separately, and fossa separately following treatment. Additionally, fixed class II appliances (Herbst and Xbow) did not result in a statistically significant positional change in condyle relative to the fossa position compared to controls. Finally, the concern that the condyles will be moved into an unphysiological position using fixed class II correctors (Herbst and Xbow) was not supported by the results of this thesis.

## References

- Aiken, A., Bouloux, G., & Hudgins, P. (2012). MR imaging of the temporomandibular joint. *Magnetic Resonance Imaging Clinics of North America*, 20(3).  
<https://doi.org/10.1016/j.mric.2012.05.002>
- al Riyami I. (2021). *Volume and shape changes of mandibular condyles in growing patients treated with fixed Class II appliances using CBCT*. University of Alberta.
- Al-Koshab, M., Nambiar, P., & John, J. (2015). Assessment of condyle and glenoid fossa morphology using CBCT in south-east Asians. *PLoS ONE*, 10(3).  
<https://doi.org/10.1371/journal.pone.0121682>
- Alomar, X., Medrano, J., Cabratosa, J., Clavero, J. A., Lorente, M., Serra, I., Monill, J. M., & Salvador, A. (2007). Anatomy of the temporomandibular joint. *Seminars in Ultrasound, CT, and MR*, 28(3). <https://doi.org/10.1053/j.sult.2007.02.002>
- Al-Saleh, M. A. Q., Alsufyani, N., Flores-Mir, C., Nebbe, B., & Major, P. W. (2015). Changes in temporomandibular joint morphology in class II patients treated with fixed mandibular repositioning and evaluated through 3D imaging: A systematic review. *Orthodontics and Craniofacial Research*, 18(4), 185–201. <https://doi.org/10.1111/ocr.12099>
- Antonopoulou, M., Iatrou, I., Paraschos, A., & Anagnostopoulou, S. (2013). Variations of the attachment of the superior head of human lateral pterygoid muscle. *Journal of Cranio-Maxillo-Facial Surgery : Official Publication of the European Association for Cranio-Maxillo-Facial Surgery*, 41(6), e91-7. <https://doi.org/10.1016/j.jcms.2012.11.021>

- Arieta-Miranda, J. M., Silva-Valencia, M., Flores-Mir, C., Paredes-Sampen, N. A., & Arriola-Guillen, L. E. (2013). Spatial analysis of condyle position according to sagittal skeletal relationship, assessed by cone beam computed tomography. *Progress in Orthodontics*, *14*(1), 1–9. <https://doi.org/10.1186/2196-1042-14-36>
- Atresh, A., Cevidanes, L. H. S., Yatabe, M., Muniz, L., Nguyen, T., Larson, B., Manton, D. J., & Schneider, P. M. (2018). Three-dimensional treatment outcomes in Class II patients with different vertical facial patterns treated with the Herbst appliance. *American Journal of Orthodontics and Dentofacial Orthopedics*, *154*(2), 238-248.e1. <https://doi.org/10.1016/j.ajodo.2017.11.037>
- Bag, A. K., Gaddikeri, S., Singhal, A., Hardin, S., Tran, B. D., Medina, J. A., & Curé, J. K. (2014). Imaging of the temporomandibular joint: An update. *World Journal of Radiology*, *6*(8). <https://doi.org/10.4329/wjr.v6.i8.567>
- Baltromejus S, Ruf S, & Pancherz H. (2002). Effective temporomandibular joint growth and chin position changes: Activator versus Herbst treatment. A cephalometric roentgenographic study. *Eur J Orthod*, 627–637.
- Barbara G. Tabachnick, & Linda S. Fidell. (2007). *Using Multivariate Statistics* (5th ed.). Pearson Education. Inc.
- Baumgaertel, S., Palomo, J. M., Palomo, L., & Hans, M. G. (2009). Reliability and accuracy of cone-beam computed tomography dental measurements. *American Journal of Orthodontics and Dentofacial Orthopedics : Official Publication of the American Association of Orthodontists, Its Constituent Societies, and the American Board of Orthodontics*, *136*(1), 19–25; discussion 25-8. <https://doi.org/10.1016/j.ajodo.2007.09.016>

- Baysal, A., & Uysal, T. (2014). Dentoskeletal effects of Twin Block and Herbst appliances in patients with Class II division 1 mandibular retrognathia. *European Journal of Orthodontics*, 36(2), 164–172. <https://doi.org/10.1093/ejo/cjt013>
- Bender, M. E., Lipin, R. B., & Goudy, S. L. (2018). Development of the Pediatric Temporomandibular Joint. In *Oral and Maxillofacial Surgery Clinics of North America* (Vol. 30, Issue 1, pp. 1–9). W.B. Saunders. <https://doi.org/10.1016/j.coms.2017.09.002>
- Bergman AA, & Heidger PM. (1996). *Histology*. Saunders Company.
- Bhutada, M. K., Phanachet, I., Whittle, T., Peck, C. C., & Murray, G. M. (2008). Regional properties of the superior head of human lateral pterygoid muscle. *European Journal of Oral Sciences*, 116(6), 518–524. <https://doi.org/10.1111/j.1600-0722.2008.00582.x>
- Buschang, P. H., & Gandini Júnior, L. G. (2002). Mandibular skeletal growth and modelling between 10 and 15 years of age. *European Journal of Orthodontics*, 24(1), 69–79. <https://doi.org/10.1093/ejo/24.1.69>
- Carpentier, P., Yung, J. P., Marguelles-Bonnet, R., & Meunissier, M. (1988). Insertions of the lateral pterygoid muscle: an anatomic study of the human temporomandibular joint. *Journal of Oral and Maxillofacial Surgery : Official Journal of the American Association of Oral and Maxillofacial Surgeons*, 46(6), 477–482. [https://doi.org/10.1016/0278-2391\(88\)90417-x](https://doi.org/10.1016/0278-2391(88)90417-x)
- Chayanupatkul A, Rabie AB, & Hägg U. (2003). *Temporomandibular response to early and late removal of bite-jumping devices*. <https://academic.oup.com/ejo/article/25/5/465/414398>

- Cheib, P. L., Cevidanes, L. H. S., Carlos de Oliveira Ruellas, A., Franchi, L., Moyses Braga, W. F., Oliveira, D., & Quiroga Souki, B. (2016). Displacement of the Mandibular Condyles Immediately after Herbst Appliance Insertion - 3D Assessment. *Turkish Journal of Orthodontics*, 29(2), 31–37. <https://doi.org/10.5152/turkjorthod.2016.160008>
- Cheib Vilefort, P. L., Farah, L. O., Gontijo, H. P., Moro, A., Ruellas, A. C. de O., Cevidanes, L. H. S., Nguyen, T., Franchi, L., McNamara, J. A., & Souki, B. Q. (2019). Condyle-glenoid fossa relationship after Herbst appliance treatment during two stages of craniofacial skeletal maturation: A retrospective study. *Orthodontics and Craniofacial Research*, 22(4), 345–353. <https://doi.org/10.1111/ocr.12338>
- Connie P. Ling. (2016). *Transverse, Vertical, and Antero-posterior changes between Tooth-borne versus Dresden Bone-borne Rapid Maxillary Expansion: A Randomized Controlled Clinical Trial*. University of Alberta.
- Currie, K., Oh, H., Flores-Mir, C., & Lagravère, M. (2020). CBCT assessment of posterior cranial base and surrounding structures in orthodontically treated adolescents. *International Orthodontics*, 18(2). <https://doi.org/10.1016/j.ortho.2020.01.004>
- Damstra, J., Fourie, Z., Huddleston Slater, J. J. R., & Ren, Y. (2011). Reliability and the smallest detectable difference of measurements on 3-dimensional cone-beam computed tomography images. *American Journal of Orthodontics and Dentofacial Orthopedics : Official Publication of the American Association of Orthodontists, Its Constituent Societies, and the American Board of Orthodontics*, 140(3). <https://doi.org/10.1016/j.ajodo.2011.02.020>

- Dandajena, T. C. (2010). Hybrid Functional Appliances for Management of Class II Malocclusions. In *Current Therapy in Orthodontics* (pp. 103–114). Elsevier.  
<https://doi.org/10.1016/B978-0-323-05460-7.00010-7>
- de Assis, F., Carvalho, R., Helena, L., Cevidanes, S., Trindade, A., da Motta, S., Antonio De Oliveira Almeida, M., & Phillips, C. (2010). Three-dimensional assessment of mandibular advancement 1 year after surgery. *Am J Orthod Dentofacial Orthop*, *137*(4 Suppl).  
<https://doi.org/10.1016/j.ajodo>
- Defabianis, P. (2001). Condylar fractures treatment in children and youths: influence on function and face development (a five year retrospective analysis). *The Functional Orthodontist*, *18*(2), 24–31.
- Defabianis, P. (2003). Post-traumatic TMJ internal derangement: impact on facial growth (findings in a pediatric age group). *The Journal of Clinical Pediatric Dentistry*, *27*(4), 297–303. <https://doi.org/10.17796/jcpd.27.4.2782236161p3p467>
- Dergin, G., Kilic, C., Gozneli, R., Yildirim, D., Garip, H., & Moroglu, S. (2012). Evaluating the correlation between the lateral pterygoid muscle attachment type and internal derangement of the temporomandibular joint with an emphasis on MR imaging findings. *Journal of Cranio-Maxillo-Facial Surgery : Official Publication of the European Association for Cranio-Maxillo-Facial Surgery*, *40*(5), 459–463. <https://doi.org/10.1016/j.jcms.2011.08.002>
- Dimitroulis, G. (1997). Condylar injuries in growing patients. *Australian Dental Journal*, *42*(6), 367–371. <https://doi.org/10.1111/j.1834-7819.1997.tb06079.x>
- D’Ippolito, S. M., Borri Wolosker, A. M., D’Ippolito, G., Herbert de Souza, B., & Fenyó-Pereira, M. (2010). Evaluation of the lateral pterygoid muscle using magnetic resonance

imaging. *Dento Maxillo Facial Radiology*, 39(8), 494–500.

<https://doi.org/10.1259/dmfr/80928433>

Durão, A. R., Pittayapat, P., Rockenbach, I. B., Olszewski, R., Ng, S., Ferreira, A. P., & Jacobs, R. (2013). Validity of 2D lateral cephalometry in orthodontics: A systematic review.

*Progress in Orthodontics*, 14(1). <https://doi.org/10.1186/2196-1042-14-31>

Farronato, G., Rosso, G., Giannini, L., Galbiati, G., & Maspero, C. (2016). Correlation between skeletal Class II and temporomandibular joint disorders: a literature review. *Minerva Stomatologica*, 65(4), 239–247.

Fichera, G., Ronsivalle, V., Santonocito, S., Aboulazm, K. S., Isola, G., Leonardi, R., & Palazzo, G. (2021). Class ii skeletal malocclusion and prevalence of temporomandibular disorders. An epidemiological pilot study on growing subjects. *Journal of Functional Morphology and Kinesiology*, 6(3). <https://doi.org/10.3390/jfmk6030063>

Flores-Mir, C., Barnett, G., Higgins, D. W., Heo, G., & Major, P. W. (2009). Short-term skeletal and dental effects of the Xbow appliance as measured on lateral cephalograms. *American Journal of Orthodontics and Dentofacial Orthopedics*, 136(6), 822–832.

<https://doi.org/10.1016/j.ajodo.2008.01.021>

Gaillard F. (2011). *Temporomandibular Joint*. <a

Href="https://Commons.Wikimedia.Org/Wiki/File:Temporomandibular\_joint.Png">Frank

Gaillard</A>, <a Href="https://Creativecommons.Org/Licenses/by-Sa/3.0">CC BY-SA

3.0</A>, via Wikimedia Commons.

Garant P. (2003). *Oral cells and tissues* (1st ed.). Quintessence Pub Co.

- Gu, S., Wu, W., Liu, C., Yang, L., Sun, C., Ye, W., Li, X., Chen, J., Long, F., & Chen, Y. (2014). BMPRIA mediated signaling is essential for temporomandibular joint development in mice. *PloS One*, 9(8). <https://doi.org/10.1371/journal.pone.0101000>
- Henrikson, T. (1999). Temporomandibular disorders and mandibular function in relation to Class II malocclusion and orthodontic treatment. A controlled, prospective and longitudinal study. *Swedish Dental Journal. Supplement*, 134.
- Higgins, & W. Duncan. (2006). "Xbow<sup>TM</sup>: Straight to the Target when Straight is the Target". *Orthodontic Perspectives*, XIII(2).
- Insabralde, N. M., Rodrigues de Almeida, M., Rodrigues de Almeida-Pedrin, R., Flores-Mir, C., & Castanha Henriques, J. F. (2021). Retrospective comparison of dental and skeletal effects in the treatment of Class II malocclusion between Herbst and Xbow appliances. *American Journal of Orthodontics and Dentofacial Orthopedics*, 160(4), 544–551. <https://doi.org/10.1016/j.ajodo.2020.05.021>
- James H. Bray, & Scott E. Maxwell. (1985). Omnibus MANOVA Tests. In *Multivariate Analysis of Variance* (pp. 14–39). SAGE Publications, Inc. <https://doi.org/10.4135/9781412985222.d16>
- Katsavrias, E. G. (2003). The effect of mandibular protrusive (activator) appliances on articular eminence morphology. *The Angle Orthodontist*, 73(6), 647–653. [https://doi.org/10.1043/0003-3219\(2003\)073<0647:TEOMPA>2.0.CO;2](https://doi.org/10.1043/0003-3219(2003)073<0647:TEOMPA>2.0.CO;2)
- Katsavrias, E. G., & Voudouris, J. C. (2004). The treatment effect of mandibular protrusive appliances on the glenoid fossa for Class II correction. *The Angle Orthodontist*, 74(1), 79–85. [https://doi.org/10.1043/0003-3219\(2004\)074<0079:TTEOMP>2.0.CO;2](https://doi.org/10.1043/0003-3219(2004)074<0079:TTEOMP>2.0.CO;2)

- Kinzinger, G., Kober, C., & Diedrich, P. (2007). Topography and morphology of the mandibular condyle during fixed functional orthopedic treatment --a magnetic resonance imaging study. *Journal of Orofacial Orthopedics = Fortschritte Der Kieferorthopadie : Organ/Official Journal Deutsche Gesellschaft Fur Kieferorthopadie*, 68(2). <https://doi.org/10.1007/s00056-007-0650-0>
- Kinzinger, G. S. M., Roth, A., Glden, N., Bcker, A., & Diedrich, P. R. (2006). Effects of orthodontic treatment with fixed functional orthopaedic appliances on the condyle-fossa relationship in the temporomandibular joint: a magnetic resonance imaging study (Part I). *Dento Maxillo Facial Radiology*, 35(5), 339–346. <https://doi.org/10.1259/dmfr/53048233>
- Koay, W. L., Yang, Y., Tse, C. S. K., & Gu, M. (2016). Effects of Two-Phase Treatment with the Herbst and Preadjusted Edgewise Appliances on the Upper Airway Dimensions. *Scientific World Journal*, 2016. <https://doi.org/10.1155/2016/4697467>
- Koo, T. K., & Li, M. Y. (2016). A Guideline of Selecting and Reporting Intraclass Correlation Coefficients for Reliability Research. *Journal of Chiropractic Medicine*, 15(2), 155–163. <https://doi.org/10.1016/j.jcm.2016.02.012>
- Kozak FK, Ospina JC, & Cardenas MF. (2015). Characteristics of normal and abnormal postnatal craniofacial growth and development. In *Cummings pediatric otolaryngology* (6th ed.). Saunders.
- Krarup, S., Darvann, T. A., Larsen, P., Marsh, J. L., & Kreiborg, S. (2005). Three-dimensional analysis of mandibular growth and tooth eruption. *Journal of Anatomy*, 207(5). <https://doi.org/10.1111/j.1469-7580.2005.00479.x>

- Krisjane, Z., Urtane, I., Krumina, G., & Zepa, K. (2009). Three-dimensional evaluation of TMJ parameters in Class II and Class III patients. In *Baltic Dental and Maxillofacial Journal* (Vol. 11, Issue 1).
- Kyburz, K. S., Eliades, T., & Papageorgiou, S. N. (2019). What effect does functional appliance treatment have on the temporomandibular joint? A systematic review with meta-analysis. In *Progress in Orthodontics* (Vol. 20, Issue 1). Springer Berlin Heidelberg.  
<https://doi.org/10.1186/s40510-019-0286-9>
- Lagravère, M. O., Carey, J., Toogood, R. W., & Major, P. W. (2008). Three-dimensional accuracy of measurements made with software on cone-beam computed tomography images. *American Journal of Orthodontics and Dentofacial Orthopedics : Official Publication of the American Association of Orthodontists, Its Constituent Societies, and the American Board of Orthodontics*, 134(1). <https://doi.org/10.1016/j.ajodo.2006.08.024>
- LeCornu, M., Cevidane, L. H. S., Zhu, H., Wu, C.-D., Larson, B., & Nguyen, T. (2013). Three-dimensional treatment outcomes in Class II patients treated with the Herbst appliance: a pilot study. *American Journal of Orthodontics and Dentofacial Orthopedics : Official Publication of the American Association of Orthodontists, Its Constituent Societies, and the American Board of Orthodontics*, 144(6). <https://doi.org/10.1016/j.ajodo.2013.07.014>
- Lee, S., & Lee, D. K. (2018). What is the proper way to apply the multiple comparison test? *Korean Journal of Anesthesiology*, 71(5), 353–360. <https://doi.org/10.4097/kja.d.18.00242>
- Li, X., Liang, W., Ye, H., Weng, X., Liu, F., Lin, P., & Liu, X. (2015). Overexpression of Indian hedgehog partially rescues short stature homeobox 2-overexpression-associated congenital

- dysplasia of the temporomandibular joint in mice. *Molecular Medicine Reports*, 12(3).  
<https://doi.org/10.3892/mmr.2015.3959>
- Li, X., Liang, W., Ye, H., Weng, X., Liu, F., & Liu, X. (2014). Overexpression of Shox2 leads to congenital dysplasia of the temporomandibular joint in mice. *International Journal of Molecular Sciences*, 15(8). <https://doi.org/10.3390/ijms150813135>
- Liberton, D. K., Verma, P., Contratto, A., & Lee, J. S. (2019). Development and Validation of Novel Three-Dimensional Craniofacial Landmarks on Cone-Beam Computed Tomography Scans. *Journal of Craniofacial Surgery*, 30(7), E611–E615.  
<https://doi.org/10.1097/SCS.0000000000005627>
- Loughner, B., Miller, J., Broumand, V., & Cooper, B. (1997). The development of strains, forces and nociceptor activity in retrodiscal tissues of the temporomandibular joint of male and female goats. *Experimental Brain Research*, 113(2). <https://doi.org/10.1007/BF02450329>
- Mallya, S. M., & Tetradis, S. (2014). Cone-Beam Computed Tomography. In *Oral Radiology* (pp. 214–228). Elsevier. <https://doi.org/10.1016/B978-0-323-09633-1.00013-4>
- Manfredi, C., Cimino, R., Trani, A., & Pancherz, H. (2001). Skeletal changes of Herbst appliance therapy investigated with more conventional cephalometrics and European norms. *The Angle Orthodontist*, 71(3), 170–176. [https://doi.org/10.1043/0003-3219\(2001\)071<0170:SCOHAT>2.0.CO;2](https://doi.org/10.1043/0003-3219(2001)071<0170:SCOHAT>2.0.CO;2)
- McLain, J. B., & Proffitt, W. R. (1985). Oral health status in the United States: prevalence of malocclusion. *Journal of Dental Education*, 49(6).

- Mérida Velasco, J. R., Rodríguez Vázquez, J. F., de la Cuadra Blanco, C., Campos López, R., Sánchez, M., & Mérida Velasco, J. A. (2009). Development of the mandibular condylar cartilage in human specimens of 10-15 weeks' gestation. *Journal of Anatomy*, 214(1). <https://doi.org/10.1111/j.1469-7580.2008.01009.x>
- Mérida-Velasco, J. R., Rodríguez-Vázquez, J. F., Mérida-Velasco, J. A., Sánchez-Montesinos, I., Espín-Ferra, J., & Jiménez-Collado, J. (1999). Development of the human temporomandibular joint. *The Anatomical Record*, 255(1). [https://doi.org/10.1002/\(SICI\)1097-0185\(19990501\)255:1<20::AID-AR4>3.0.CO;2-N](https://doi.org/10.1002/(SICI)1097-0185(19990501)255:1<20::AID-AR4>3.0.CO;2-N)
- Michelotti, A., & Iodice, G. (2010). The role of orthodontics in temporomandibular disorders. *Journal of Oral Rehabilitation*, 37(6), 411–429. <https://doi.org/10.1111/j.1365-2842.2010.02087.x>
- Milam, S. B. (2005). Pathogenesis of degenerative temporomandibular joint arthritides. *Odontology*, 93(1), 7–15. <https://doi.org/10.1007/s10266-005-0056-7>
- Mizoguchi, I., Nakamura, M., Takahashi, I., Kagayama, M., & Mitani, H. (1992). A comparison of the immunohistochemical localization of type I and type II collagens in craniofacial cartilages of the rat. *Acta Anatomica*, 144(1), 59–64. <https://doi.org/10.1159/000147286>
- Moerenhout, B. A. M. M. L., Gelaude, F., Swennen, G. R. J., Casselman, J. W., van der Sloten, J., & Mommaerts, M. Y. (2009). Accuracy and repeatability of cone-beam computed tomography (CBCT) measurements used in the determination of facial indices in the laboratory setup. *Journal of Cranio-Maxillo-Facial Surgery : Official Publication of the European Association for Cranio-Maxillo-Facial Surgery*, 37(1). <https://doi.org/10.1016/j.jcms.2008.07.006>

Mohlin, B., Axelsson, S., Paulin, G., Pietilä, T., Bondemark, L., Brattströ, V., Hansen, K., & Holm, A.-K. (2007). TMD in Relation to Malocclusion and Orthodontic Treatment A Systematic Review. *Angle Orthodontist*, 77(3), 542. <https://doi.org/10.2319/033006-129>

Nimon, K. F. (2012). Statistical Assumptions of Substantive Analyses Across the General Linear Model: A Mini-Review. *Frontiers in Psychology*, 3. <https://doi.org/10.3389/fpsyg.2012.00322>

O'Brien, K., Wright, J., Conboy, F., Sanjie, Y., Mandall, N., Chadwick, S., Connolly, I., Cook, P., Birnie, D., Hammond, M., Harradine, N., Lewis, D., McDade, C., Mitchell, L., Murray, A., O'Neill, J., Read, M., Robinson, S., Roberts-Harry, D., Shaw, I. (2003). Effectiveness of treatment for Class II malocclusion with the Herbst or twin-block appliances: a randomized, controlled trial. *American Journal of Orthodontics and Dentofacial Orthopedics : Official Publication of the American Association of Orthodontists, Its Constituent Societies, and the American Board of Orthodontics*, 124(2), 128–137. [https://doi.org/10.1016/s0889-5406\(03\)00345-7](https://doi.org/10.1016/s0889-5406(03)00345-7)

Omami, G., & Lurie, A. (2012). Magnetic resonance imaging evaluation of discal attachment of superior head of lateral pterygoid muscle in individuals with symptomatic temporomandibular joint. *Oral Surgery, Oral Medicine, Oral Pathology and Oral Radiology*, 114(5), 650–657. <https://doi.org/10.1016/j.oooo.2012.07.482>

Owtad, P., Potres, Z., Shen, G., Petocz, P., & Darendeliler, M. A. (2011). A histochemical study on condylar cartilage and glenoid fossa during mandibular advancement. *The Angle Orthodontist*, 81(2). <https://doi.org/10.2319/021710-99.1>

- Oz, U., Orhan, K., & Abe, N. (2011). Comparison of linear and angular measurements using two-dimensional conventional methods and three-dimensional cone beam CT images reconstructed from a volumetric rendering program in vivo. *Dento Maxillo Facial Radiology*, 40(8). <https://doi.org/10.1259/dmfr/15644321>
- Oztoprak, M. O., Nalbantgil, D., Uyanlar, A., & Arun, T. (2012). A cephalometric comparative study of class II correction with Sabbagh Universal Spring (SUS(2)) and Forsus FRD appliances. *European Journal of Dentistry*, 6(3), 302–310.
- Pancherz, H. (1979). Treatment of Class II malocclusions by jumping the bite with the Herbst appliance. *American Journal of Orthodontics*, 76(4), 423–442.  
[https://doi.org/10.1016/0002-9416\(79\)90227-6](https://doi.org/10.1016/0002-9416(79)90227-6)
- Pancherz, H. (2003). History, Background, and Development of the Herbst Appliance. In *Seminars in Orthodontics* (Vol. 9, Issue 1).
- Pancherz, H., & Michailidou, C. (2004). Temporomandibular joint growth changes in hyperdivergent and hypodivergent Herbst subjects. A long-term roentgenographic cephalometric study. *American Journal of Orthodontics and Dentofacial Orthopedics : Official Publication of the American Association of Orthodontists, Its Constituent Societies, and the American Board of Orthodontics*, 126(2).  
<https://doi.org/10.1016/j.ajodo.2003.07.015>
- Pancherz, H., Ruf, S., & Thomalske-Faubert, C. (1999). Mandibular articular disk position changes during Herbst treatment: a prospective longitudinal MRI study. *American Journal of Orthodontics and Dentofacial Orthopedics : Official Publication of the American*

*Association of Orthodontists, Its Constituent Societies, and the American Board of Orthodontics*, 116(2). [https://doi.org/10.1016/s0889-5406\(99\)70219-2](https://doi.org/10.1016/s0889-5406(99)70219-2)

Papadopoulos MA. (2006). *Orthodontic Treatment of the Class II Noncompliant Patient*.

Papageorgiou, S. N., Koretsi, V., & Jäger, A. (2017). Bias from historical control groups used in orthodontic research: a meta-epidemiological study. *European Journal of Orthodontics*, 39(1), 98–105. <https://doi.org/10.1093/ejo/cjw035>

Park, Y., Chen, S., Ahmad, N., Hayami, T., & Kapila, S. (2019). Estrogen Selectively Enhances TMJ Disc but Not Knee Meniscus Matrix Loss. *Journal of Dental Research*, 98(13), 1532–1538. <https://doi.org/10.1177/0022034519875956>

Pauwels, R., Araki, K., Siewerdsen, J. H., & Thongvigitmanee, S. S. (2015). Technical aspects of dental CBCT: State of the art. In *Dentomaxillofacial Radiology* (Vol. 44, Issue 1). British Institute of Radiology. <https://doi.org/10.1259/dmfr.20140224>

Popowich, K., Nebbe, B., & Major, P. W. (2003). Effect of Herbst treatment on temporomandibular joint morphology: a systematic literature review. *American Journal of Orthodontics and Dentofacial Orthopedics : Official Publication of the American Association of Orthodontists, Its Constituent Societies, and the American Board of Orthodontics*, 123(4). <https://doi.org/10.1067/mod.2003.89>

Portney LG, & Watkins MP. (2000). *Foundations of clinical research: applications to practice* (2nd ed.). Pearson.

Proffit W, Fields H, & Sarver D. (2012). *Contemporary Orthodontics* (5th ed.). Mosby.

- Proffit, W. R., Fields, H. W., & Moray, L. J. (1998). Prevalence of malocclusion and orthodontic treatment need in the United States: estimates from the NHANES III survey. *The International Journal of Adult Orthodontics and Orthognathic Surgery*, 13(2), 97–106.
- Rabie, A. B., Zhao, Z., Shen, G., Hägg, E. U., Dr, O., & Robinson, W. (2001). Osteogenesis in the glenoid fossa in response to mandibular advancement. *American Journal of Orthodontics and Dentofacial Orthopedics : Official Publication of the American Association of Orthodontists, Its Constituent Societies, and the American Board of Orthodontics*, 119(4), 390–400. <https://doi.org/10.1067/mod.2001.112875>
- Randeep S. Chana. (2013). *Cephalometric Evaluation of Dental Class II Correction Using the Xbow® Appliance in Different Facial Patterns* . University of Manitoba.
- Ritto, A. K., & Ferreira, A. P. (2000). Fixed functional appliances--a classification. *The Functional Orthodontist*, 17(2), 12–30, 32.
- Rodrigues, A. F., Fraga, M. R., & Vitral, R. W. F. (2009a). Computed tomography evaluation of the temporomandibular joint in Class I malocclusion patients: condylar symmetry and condyle-fossa relationship. *American Journal of Orthodontics and Dentofacial Orthopedics : Official Publication of the American Association of Orthodontists, Its Constituent Societies, and the American Board of Orthodontics*, 136(2). <https://doi.org/10.1016/j.ajodo.2007.07.032>
- Rodrigues, A. F., Fraga, M. R., & Vitral, R. W. F. (2009b). Computed tomography evaluation of the temporomandibular joint in Class II Division 1 and Class III malocclusion patients: condylar symmetry and condyle-fossa relationship. *American Journal of Orthodontics and Dentofacial Orthopedics : Official Publication of the American Association of*

*Orthodontists, Its Constituent Societies, and the American Board of Orthodontics*, 136(2).  
<https://doi.org/10.1016/j.ajodo.2007.07.033>

Ruf, S., & Pancherz, H. (1998). Temporomandibular joint growth adaptation in Herbst treatment: a prospective magnetic resonance imaging and cephalometric roentgenographic study.

*European Journal of Orthodontics*, 20(4), 375–388. <https://doi.org/10.1093/ejo/20.4.375>

Scarfe, W. C., & Farman, A. G. (2014a). Cone-Beam Computed Tomography. In *Oral Radiology* (pp. 199–213). Elsevier. <https://doi.org/10.1016/B978-0-323-09633-1.00012-2>

Scarfe, W. C., & Farman, A. G. (2014b). Cone-Beam Computed Tomography. In *Oral Radiology* (pp. 185–198). Elsevier. <https://doi.org/10.1016/B978-0-323-09633-1.00011-0>

Seligman, D. A., & Pullinger, A. G. (1996). A multiple stepwise logistic regression analysis of trauma history and 16 other history and dental cofactors in females with temporomandibular disorders. *Journal of Orofacial Pain*, 10(4), 351–361.

Sharma, N., Singh, A., Pandey, A., Verma, V., & Singh, S. (2015). Temporomandibular joint dislocation. *National Journal of Maxillofacial Surgery*, 6(1), 16.  
<https://doi.org/10.4103/0975-5950.168212>

Shen, G., & Darendeliler, M. A. (2005). The adaptive remodeling of condylar cartilage---a transition from chondrogenesis to osteogenesis. *Journal of Dental Research*, 84(8), 691–699. <https://doi.org/10.1177/154405910508400802>

Shen, G., Hägg, U., & Darendeliler, M. (2005). Skeletal effects of bite jumping therapy on the mandible - removable vs. fixed functional appliances. *Orthodontics & Craniofacial Research*, 8(1), 2–10. <https://doi.org/10.1111/j.1601-6343.2004.00307.x>

- Sinnatamby, C. S. (2011). *Lasts Anatomy* (12th ed.).
- Smartt, J. M., Low, D. W., & Bartlett, S. P. (2005). The pediatric mandible: I. A primer on growth and development. *Plastic and Reconstructive Surgery*, *116*(1).  
<https://doi.org/10.1097/01.prs.0000169940.69315.9c>
- Souki, B. Q., Vilefort, P. L. C., Oliveira, D. D., Andrade, I., Ruellas, A. C., Yatabe, M. S., Nguyen, T., Franchi, L., McNamara, J. A., & Cevidanes, L. H. S. (2017). Three-dimensional skeletal mandibular changes associated with Herbst appliance treatment. *Orthodontics and Craniofacial Research*, *20*(2), 111–118. <https://doi.org/10.1111/ocr.12154>
- Talic, N. F. (2011). Adverse effects of orthodontic treatment: A clinical perspective. In *Saudi Dental Journal* (Vol. 23, Issue 2, pp. 55–59). <https://doi.org/10.1016/j.sdentj.2011.01.003>
- Tamimi D, & Hatcher DC. (2016). *Specialty Imaging: Temporomandibular Joint* (1st ed.). Elsevier.
- Taskaya-Yilmaz, N., Ceylan, G., Incesu, L., & Muglali, M. (2005). A possible etiology of the internal derangement of the temporomandibular joint based on the MRI observations of the lateral pterygoid muscle. *Surgical and Radiologic Anatomy : SRA*, *27*(1), 19–24.  
<https://doi.org/10.1007/s00276-004-0267-6>
- Voudouris, J. C., Woodside, D. G., Altuna, G., Angelopoulos, G., Bourque, P. J., & Lacouture, C. Y. (2003). Condyle-fossa modifications and muscle interactions during Herbst treatment, Part 2. Results and conclusions. *American Journal of Orthodontics and Dentofacial Orthopedics*, *124*(1), 13–29. [https://doi.org/10.1016/S0889-5406\(03\)00150-1](https://doi.org/10.1016/S0889-5406(03)00150-1)

- Wadhwa, S., & Kapila, S. (2008). TMJ disorders: future innovations in diagnostics and therapeutics. *Journal of Dental Education*, 72(8).
- Wang, Y., Liu, C., Rohr, J., Liu, H., He, F., Yu, J., Sun, C., Li, L., Gu, S., & Chen, Y. (2011). Tissue interaction is required for glenoid fossa development during temporomandibular joint formation. *Developmental Dynamics : An Official Publication of the American Association of Anatomists*, 240(11). <https://doi.org/10.1002/dvdy.22748>
- Yamaki, Y., Tsuchikawa, K., Nagasawa, T., & Hiroyasu, K. (2005). Embryological study of the development of the rat temporomandibular joint: highlighting the development of the glenoid fossa. *Odontology*, 93(1). <https://doi.org/10.1007/s10266-005-0046-9>
- Yokohama-Tamaki, T., Maeda, T., Tanaka, T. S., & Shibata, S. (2011). Functional analysis of CTRP3/cartducin in Meckel's cartilage and developing condylar cartilage in the fetal mouse mandible. *Journal of Anatomy*, 218(5). <https://doi.org/10.1111/j.1469-7580.2011.01354.x>
- Yun, P.-Y., & Kim, Y.-K. (2005). The role of facial trauma as a possible etiologic factor in temporomandibular joint disorder. *Journal of Oral and Maxillofacial Surgery : Official Journal of the American Association of Oral and Maxillofacial Surgeons*, 63(11), 1576–1583. <https://doi.org/10.1016/j.joms.2005.05.318>

## Appendix

Figure A2.1. Summary information about AVIZO LITE© Berlin, Thermo Fisher Science 2019.

AVIZO LITE© is a general-purpose commercial software tool for modularly viewing and analyzing scientific and industrial data, providing modules and data objects as the system's fundamental components. Modules are used to represent data items or execute computations visually. In the Project View, the components are represented by little icons. The icons are linked by lines that indicate the components' processing dependencies. Modules are formed automatically from file input data during file reading or module calculations. Modules that match an existing data object are produced using a context-sensitive popup menu as instances of certain module types. Commands may be executed manually in a separate terminal window or read from a script file (*Users-Guide-Avizo-Software-2019*, 2019).

A 3D graphics window takes up the majority of the screen. Additional three-dimensional views may be developed as needed. There are over 270 different data objects and module kinds that can be created. They enable the system to be employed in a wide variety of situations. Scripting may be used to automate and customize processes. The Avizo© developer version enables user-defined extensions. It is produced by Thermo Fisher Scientific and was initially conceived and developed under the name Amira by the Zuse Institute Berlin (ZIB) Visualization and Data Analysis Group. Avizo was launched commercially in November 2007 (*Users-Guide-Avizo-Software-2019*, 2019).

Figure A2.2 Sample size calculation.

Sample size calculation was performed with the following sample size equation:

$$n_1 = \frac{(\sigma_1^2 + \sigma_2^2) (z_{1-\alpha/2} + z_{1-\beta})^2}{\Delta^2}$$

A proportional variation measure of the anterior distance of the condyles in Class II patients was calculated in a previous study (Arieta-Miranda et al., 2013). Based on Arieta-Miranda et al., a standard deviation of 0.74 mm can be used. With an alpha of 5% and a power of 0.95, a sample size of 14 in each group was required to identify condylar positional alterations of more than 1.1 mm (clinically significant difference; see the clinical significance section).

Figure A2.3 The formulas and methodology for generation of the planes and measuring the orthogonal distance from each landmark to each plane (Sagittal, Axial, and Coronal).

In a known three points value  $P1 = (x1, y1, z1)$ ,  $P2 = (x2, y2, z2)$ ,  $P3 = (x3, y3, z3)$

Plane formula is:  $ax+by+cz+d=0$

The value of a, b, c, and d are important to calculate the perpendicular distance from a landmark point ( $P0 (x0, y0, z0)$ ) to a plane. The following equations were used to calculate these variables:

$$a = (y2 - y1) (z1 - z3) - (z2 - z1) (y1 - y3)$$

$$b = (z2 - z1) (x1 - x3) - (x2 - x1) (z1 - z3)$$

$$c = (x2 - x1) (y1 - y3) - (y2 - y1) (x1 - x3)$$

$$\text{Thus, } d = - (ax1 + by1 + cz1)$$

The perpendicular distances (the shortest distance) to a relative plane were calculated for each selected landmark using the following equation:

In a known  $P0 (x0, y0, z0)$ .

$$D = \frac{ax_0 + by_0 + cz_0 + d}{\sqrt{a^2 + b^2 + c^2}}.$$

Table A3.1 Measurement error difference average in each landmark relative to each plane in millimetres and standard deviation (SD). Please notice that the values were rounded to the first decimal place in mm. The mean difference in distance from the Right Postero-lateral Glenoid Fossa to the coronal plane showed the lowest measurement error (0.3 mm; standard deviation (SD): 0.2). However, the Right Lateral Condyle measurement error to the axial plane, and the Right Medial Condyle to the axial plane, showed the highest measurement error (1.2 mm, SD: 0.8; 1.1 mm, SD: 0.8 retrospectively).

Number	Landmarks used	The difference in mean of distances to Sagittal plane mm (SD)	The difference in mean of distances to Axial plane mm (SD)	The difference in mean of distances to Coronal plane mm (SD)
1	Right Lateral Condyle	0.5 (0.3)	1.2 (0.8)	0.6 (0.3)
2	Right Medial Condyle	0.6 (0.3)	1.1 (0.8)	0.5 (0.4)
3	Right Posterior Condyle	0.6 (0.3)	1 (0.6)	0.4 (0.1)
4	Right Antero-lateral Glenoid Fossa	0.6 (0.3)	0.9 (0.5)	0.5 (0.3)
5	Right Postero-lateral Glenoid Fossa	0.8 (0.3)	0.7 (0.4)	0.3 (0.2)
6	Right Medial Glenoid Fossa	0.7 (0.4)	1 (0.9)	0.4 (0.1)
7	Left Lateral Condyle	0.6 (0.2)	0.8 (0.8)	0.5 (0.3)
8	Left Medial Condyle	0.6 (0.3)	0.8 (0.8)	0.6 (0.3)
9	Left Posterior Condyle	0.7 (0.3)	0.9 (0.7)	0.4 (0.3)
10	Left Antero-lateral Glenoid Fossa	0.7 (0.5)	0.8 (0.8)	0.5 (0.3)
11	Left Postero-lateral Glenoid Fossa	0.8 (0.4)	0.9 (0.9)	0.4 (0.3)

12	Left Medial Glenoid Fossa	0.9 (0.3)	0.6 (0.7)	0.5 (0.3)
----	------------------------------	-----------	-----------	-----------

Table A3.2 Measurement error average of each landmark point in each axis in millimetres and standard deviation (SD). Please notice that the values were rounded to the first decimal place in mm.

Landmark	The difference in mean on X-axis in mm (SD)	The difference in mean on Y-axis in mm (SD)	The difference in mean on the Z-axis in mm (SD)
1- Foramen Magnum (FM)	0.6 (0.3)	0.5 (0.2)	0.1 (0.0)
2- Right Foramen Ovale (RFO)	0.4 (0.3)	0.9 (0.5)	0.4 (0.5)
3- Left Foramen Ovale (LFO)	0.5 (0.3)	0.6 (0.4)	0.4 (0.6)
4- Nasion (N)	0.3 (0.2)	0.2 (0.2)	0.6 (0.4)
5- Midpoint between the two-Infraorbital foramen (MIOF)	0.1 (0.1)	0.1 (0.1)	0.1 (0.1)
6- Right Infraorbital Foramen (RIO)	0.1 (0.1)	0.2 (0.1)	0.2 (0.1)
7- Left Infraorbital Foramen (LIO)	0.2 (0.1)	0.2 (0.1)	0.2 (0.1)
8- Right Lateral Condyle (RLC)	0.2 (0.2)	0.4 (0.2)	0.5 (0.4)
9- Right Medial Condyle (RMC)	0.1 (0.1)	0.4 (0.2)	0.5 (0.4)
10- Right Posterior Condyle (RPC)	0.4 (0.1)	0.1 (0.1)	0.6 (0.4)
11- Right Antero-lateral Glenoid Fossa (RALGF)	0.4 (0.2)	0.4 (0.2)	0 (0.1)

12- Right Postero-lateral Glenoid Fossa (RPLGF)	0.3 (0.2)	0 (0)	0.2 (0)
13- Right Medial Glenoid Fossa (RMGF)	0.3 (0.2)	0.1 (0.1)	0.1 (0.1)
14- Left Lateral Condyle (LLC)	0.1 (0.1)	0.3 (0.2)	0.3 (0.2)
15- Left Medial Condyle (LMC)	0.1 (0.1)	0.4 (0.3)	0.4 (0.3)
16- Left Posterior Condyle (LPC)	0.3 (0.2)	0.1 (0.1)	0.5 (0.2)
17- Left Antero-lateral Glenoid Fossa (LALGF)	0.6 (0.6)	0.4 (0.1)	0 (0.1)
18- Left Postero-lateral Glenoid Fossa (LPLGF)	0.4 (0.2)	0 (0.1)	0.3 (0.2)
19- Left Medial Glenoid Fossa (LMGF)	0.6 (0.4)	0.4 (0.2)	0.1 (0.1)

Table A3.3 The variables that represent landmarks corresponding to each plane of the groups. Showing the number of test subjects, mean (in mm), standard deviation (in mm), and minimum and maximum value (in mm). The values were rounded to the second decimal place in mm.

Variable (landmark-plane)	Treatment group	Number of cases	Mean	Std. Deviation	Minimum	Maximum
RLC_Coronal	Control	18	0.67	0.82	-0.61	2.20
	Herbst	17	0.20	1.15	-1.83	2.29
	Xbow	19	0.96	1.01	-0.92	2.62
RLC_Axial	Control	18	0.46	0.91	-1.18	2.17
	Herbst	17	-0.25	0.59	-1.39	0.83
	Xbow	19	-0.24	0.97	-1.98	1.26
RLC_Sagittal	Control	18	0.66	0.65	-0.23	1.73
	Herbst	17	0.66	0.29	0.15	1.35
	Xbow	19	0.55	0.58	-0.54	1.61

RMC_Coronal	Control	18	0.78	1.71	-2.68	4.84
	Herbst	17	0.18	1.60	-3.14	2.83
	Xbow	19	1.16	1.37	-0.61	4.06
RMC_Axial	Control	18	0.47	1.23	-1.41	2.96
	Herbst	17	-0.27	0.79	-1.58	1.18
	Xbow	19	0.39	0.99	-1.19	2.65
RMC_Sagittal	Control	18	0.36	0.64	-0.72	1.66
	Herbst	17	0.33	0.57	-0.80	1.31
	Xbow	19	0.39	0.62	-0.46	1.48
RPC_Coronal	Control	18	0.80	1.30	-1.69	3.08
	Herbst	17	-0.06	1.27	-2.34	2.26
	Xbow	19	1.05	0.90	-0.66	2.43

RPC_Axial	Control	18	0.48	1.07	-1.45	2.49
	Herbst	17	-0.12	1.21	-2.48	1.79
	Xbow	19	0.46	1.09	-0.92	2.81
RPC_Sagittal	Control	18	0.75	0.72	-0.23	2.34
	Herbst	17	0.39	0.95	-1.25	1.99
	Xbow	19	0.51	1.03	-1.58	2.40
RALGF_Coronal	Control	18	0.33	1.10	-2.27	2.71
	Herbst	17	0.00	1.05	-1.84	2.01
	Xbow	19	0.31	1.06	-1.68	1.87
RALGF_Axial	Control	18	0.25	0.83	-1.28	2.18
	Herbst	17	0.43	0.44	-0.42	1.30
	Xbow	19	-0.06	0.85	-1.23	1.40

RALGF_Sagittal	Control	18	0.70	0.97	-0.61	3.01
	Herbst	17	0.68	0.87	-0.68	2.74
	Xbow	19	0.52	0.90	-0.99	2.09
RPLGF_Coronal	Control	18	0.67	0.73	-0.82	1.69
	Herbst	17	0.21	0.38	-0.35	0.93
	Xbow	19	0.61	0.85	-0.59	2.33
RPLGF_Axial	Control	18	0.21	0.76	-1.39	1.42
	Herbst	17	-0.20	0.85	-1.73	1.16
	Xbow	19	0.03	0.95	-1.31	1.65
RPLGF_Sagittal	Control	18	0.45	0.96	-1.74	1.77
	Herbst	17	0.51	0.80	-0.76	1.77
	Xbow	19	0.47	0.88	-1.35	2.12

RMGF_Coronal	Control	18	0.62	0.66	-0.70	2.02
	Herbst	17	0.27	0.86	-1.05	1.94
	Xbow	19	0.70	0.80	-0.57	1.98
RMGF_Axial	Control	18	0.05	0.69	-0.91	1.72
	Herbst	17	-0.19	0.75	-1.10	1.13
	Xbow	19	0.00	0.59	-1.06	1.08
RMGF_Sagittal	Control	18	0.57	1.17	-1.44	2.59
	Herbst	17	0.10	0.95	-1.41	1.78
	Xbow	19	0.23	0.48	-0.55	1.08
LLC_Coronal	Control	18	0.91	1.82	-2.86	4.29
	Herbst	17	0.62	1.58	-1.67	3.57
	Xbow	19	0.74	1.35	-1.78	3.19

LLC_Axial	Control	18	0.10	1.63	-2.26	3.43
	Herbst	17	-0.05	1.27	-2.25	1.80
	Xbow	19	0.47	1.00	-1.55	2.59
LLC_Sagittal	Control	18	0.72	0.64	-0.25	1.98
	Herbst	17	0.49	0.23	0.07	0.93
	Xbow	19	0.79	0.70	-0.12	2.33
LMC_Coronal	Control	18	0.72	1.16	-1.41	2.98
	Herbst	17	0.32	1.54	-2.82	3.01
	Xbow	19	1.13	1.31	-1.02	4.10
LMC_Axial	Control	18	0.53	1.17	-2.10	2.19
	Herbst	17	0.11	1.23	-2.37	2.64
	Xbow	19	0.37	1.27	-1.42	3.44

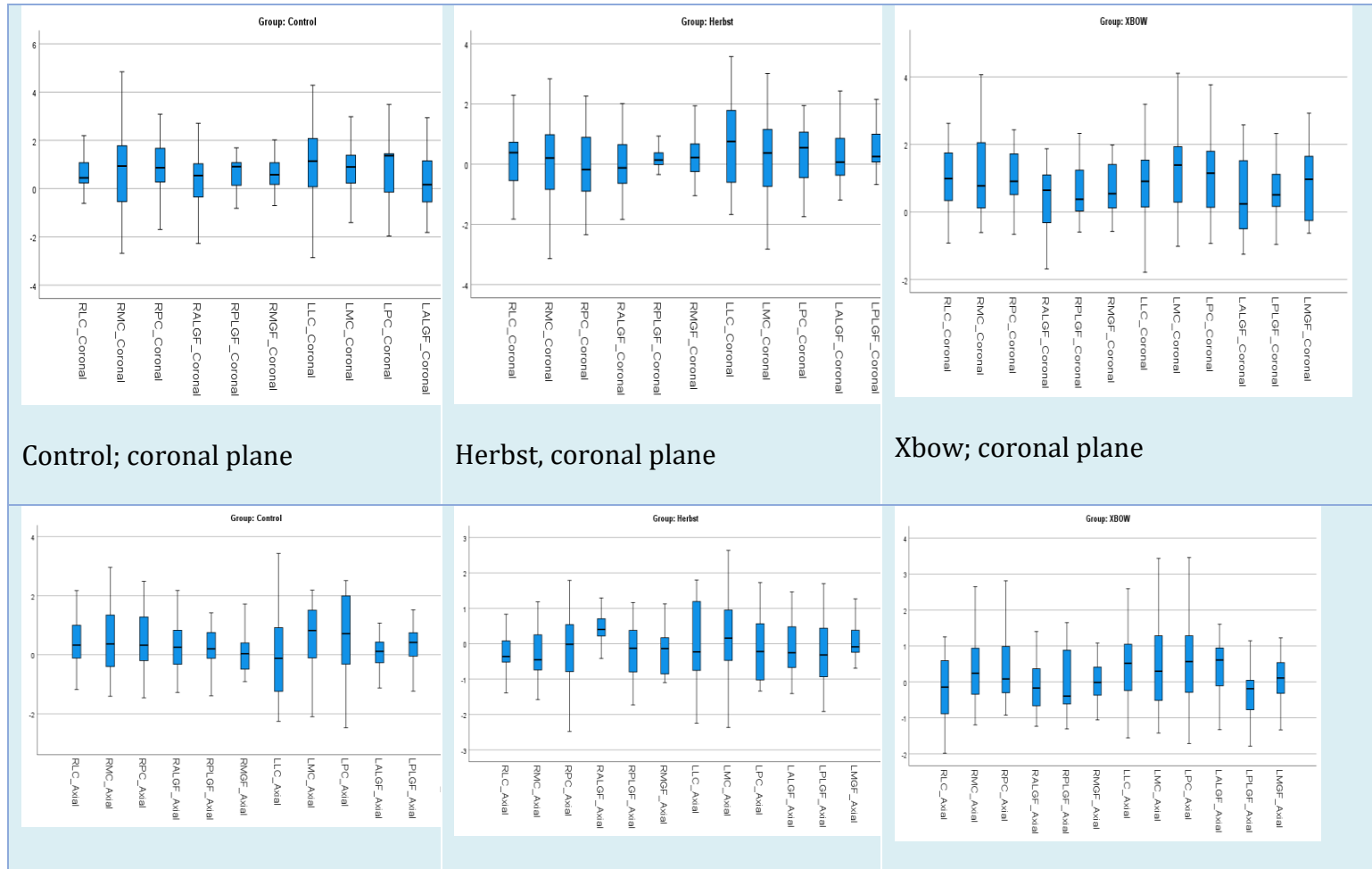
LMC_Sagittal	Control	18	0.38	0.73	-0.85	1.69
	Herbst	17	0.33	0.77	-1.03	1.74
	Xbow	19	0.56	0.80	-1.14	1.71
LPC_Coronal	Control	18	0.85	1.36	-1.96	3.49
	Herbst	17	0.30	1.15	-1.74	1.95
	Xbow	19	1.05	1.21	-0.93	3.77
LPC_Axial	Control	18	0.67	1.40	-2.47	2.51
	Herbst	17	-0.07	0.99	-1.34	1.73
	Xbow	19	0.55	1.25	-1.71	3.46
LPC_Sagittal	Control	18	0.41	0.80	-0.80	1.97
	Herbst	17	0.21	1.08	-1.82	1.53
	Xbow	19	0.24	0.74	-1.20	1.82

LALGF_Coronal	Control	18	0.44	1.33	-1.81	2.94
	Herbst	17	0.27	0.97	-1.19	2.43
	Xbow	19	0.47	1.10	-1.25	2.58
LALGF_Axial	Control	18	0.09	0.62	-1.13	1.07
	Herbst	17	-0.13	0.86	-1.41	1.46
	Xbow	19	0.46	0.77	-1.32	1.61
LALGF_Sagittal	Control	18	0.59	1.07	-1.68	2.41
	Herbst	17	0.47	0.55	-0.51	1.34
	Xbow	19	0.96	1.09	-0.74	3.14
LPLGF_Coronal	Control	18	0.71	0.83	-0.53	2.10
	Herbst	17	0.45	0.79	-0.68	2.15
	Xbow	19	0.61	0.88	-0.96	2.32

LPLGF_Axial	Control	18	0.37	0.66	-1.23	1.52
	Herbst	17	-0.28	0.99	-1.91	1.70
	Xbow	19	-0.32	0.69	-1.78	1.14
LPLGF_Sagittal	Control	18	0.69	0.72	-1.11	1.72
	Herbst	17	0.27	0.65	-1.09	1.34
	Xbow	19	0.65	1.12	-1.27	2.48
LMGF_Coronal	Control	18	0.61	0.97	-1.68	2.12
	Herbst	17	0.61	0.89	-1.14	2.17
	Xbow	19	0.80	1.05	-0.63	2.92
LMGF_Axial	Control	18	0.20	0.60	-0.82	1.47
	Herbst	17	0.07	0.56	-0.69	1.27
	Xbow	19	0.07	0.74	-1.33	1.23

LMGF_Sagittal	Control	18	0.04	0.87	-1.56	2.13
	Herbst	17	0.35	1.02	-1.25	2.23
	Xbow	19	0.51	1.09	-1.41	2.42

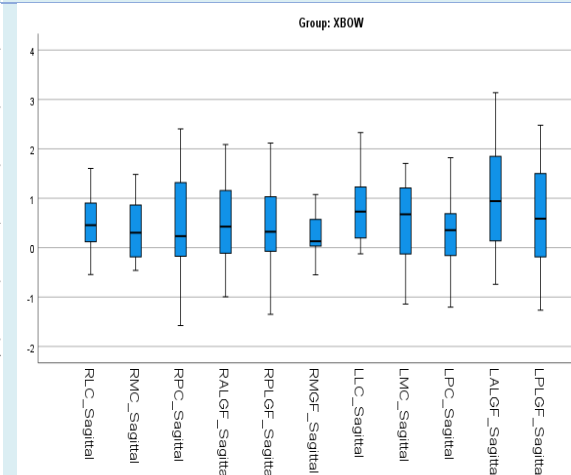
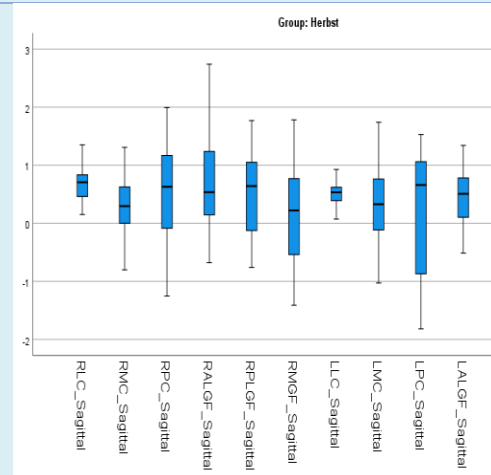
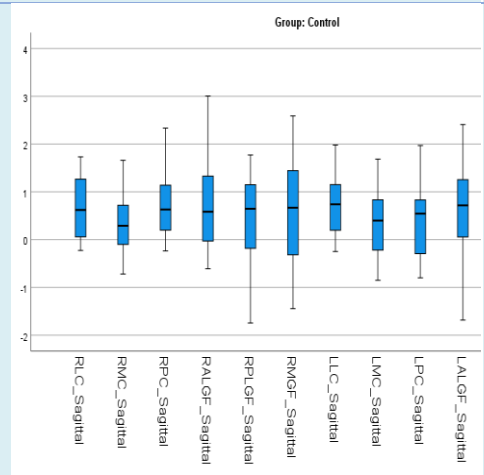
Figure A3.1 Boxplots of all dependent variables (mean difference in distance of the 12 landmarks between T0 and T1 timelines corresponding to each plane) in each group (Control, Herbst and Xbow). The X-axis represents each landmark corresponding to each plane. Y-axis represents orthogonal variation in distance between T0 and T1 in mm.



Control; axial plane

Herbst; axial plane

Xbow; axial plane



Control; sagittal plane

Herbst; sagittal plane

Xbow; sagittal plane

Figure A3.2 Scatterplot matrices of each pair of dependent variables (mean difference in distance of the 12 landmarks between T0 and T1 timelines corresponding to each plane) in each group (control, Herbst and Xbow).

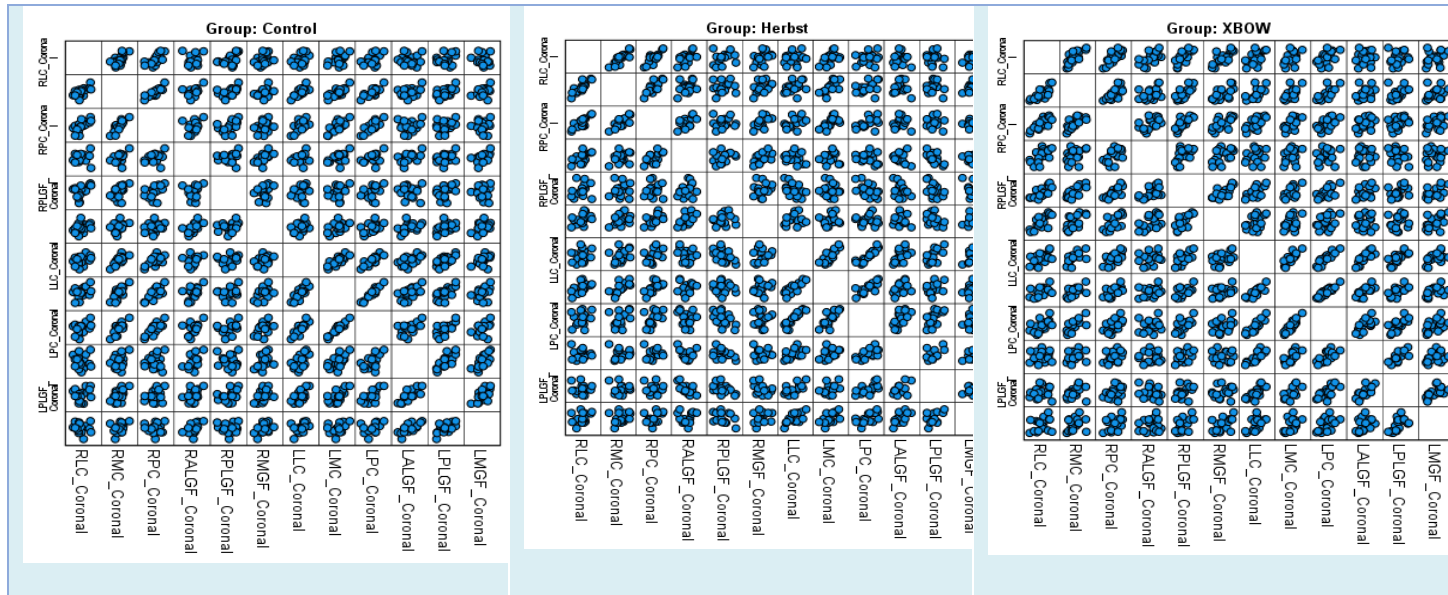


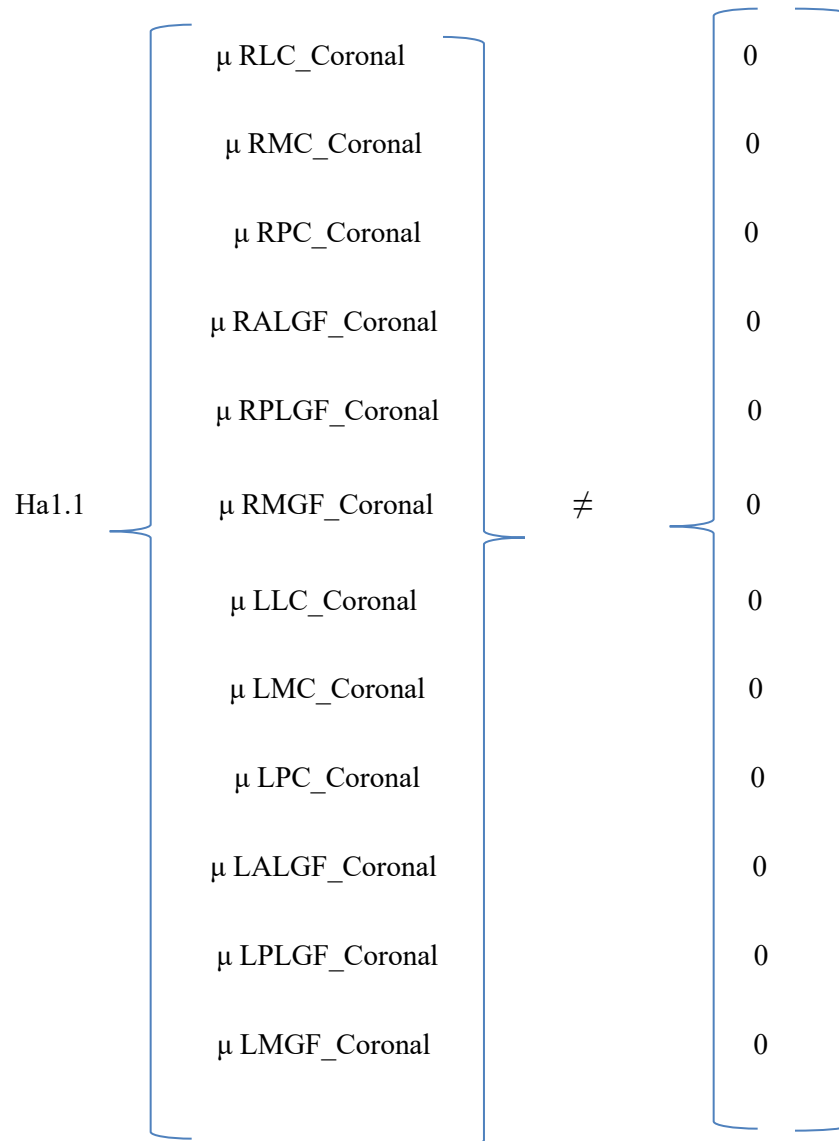


Figure A3.3 Matrices that express hypotheses of each MANOVA test.

1- Concerning the anteroposterior positional change:

- Condyle and glenoid fossa

$$H_{01.1} \left[ \begin{array}{c} \mu \text{ RLC\_Coronal} \\ \mu \text{ RMC\_Coronal} \\ \mu \text{ RPC\_Coronal} \\ \mu \text{ RALGF\_Coronal} \\ \mu \text{ RPLGF\_Coronal} \\ \mu \text{ RMGF\_Coronal} \\ \mu \text{ LLC\_Coronal} \\ \mu \text{ LMC\_Coronal} \\ \mu \text{ LPC\_Coronal} \\ \mu \text{ LALGF\_Coronal} \\ \mu \text{ LPLGF\_Coronal} \\ \mu \text{ LMGF\_Coronal} \end{array} \right] = \left[ \begin{array}{c} 0 \\ 0 \\ 0 \\ 0 \\ 0 \\ 0 \\ 0 \\ 0 \\ 0 \\ 0 \\ 0 \\ 0 \end{array} \right]$$



- Concerning the condyle:

$$\text{H01.2} \left\{ \begin{array}{l} \mu \text{ RLC\_Coronal} \\ \mu \text{ RMC\_Coronal} \\ \mu \text{ RPC\_Coronal} \\ \mu \text{ LLC\_Coronal} \\ \mu \text{ LMC\_Coronal} \\ \mu \text{ LPC\_Coronal} \end{array} \right\} = \left\{ \begin{array}{l} 0 \\ 0 \\ 0 \\ 0 \\ 0 \\ 0 \end{array} \right\}$$

$$\text{Ha1.2} \left\{ \begin{array}{l} \mu \text{ RLC\_Coronal} \\ \mu \text{ RMC\_Coronal} \\ \mu \text{ RPC\_Coronal} \\ \mu \text{ LLC\_Coronal} \\ \mu \text{ LMC\_Coronal} \\ \mu \text{ LPC\_Coronal} \end{array} \right\} \neq \left\{ \begin{array}{l} 0 \\ 0 \\ 0 \\ 0 \\ 0 \\ 0 \end{array} \right\}$$

- Concerning the glenoid fossa:

$$\text{H01.3} \left\{ \begin{array}{l} \mu \text{ RALGF\_Coronal} \\ \mu \text{ RPLGF\_Coronal} \\ \mu \text{ RMGF\_Coronal} \\ \mu \text{ LALGF\_Coronal} \\ \mu \text{ LPLGF\_Coronal} \\ \mu \text{ LMGF\_Coronal} \end{array} \right\} = \left\{ \begin{array}{l} 0 \\ 0 \\ 0 \\ 0 \\ 0 \\ 0 \end{array} \right\}$$

$$\text{Ha1.3} \left\{ \begin{array}{l} \mu \text{ RALGF\_Coronal} \\ \mu \text{ RPLGF\_Coronal} \\ \mu \text{ RMGF\_Coronal} \\ \mu \text{ LALGF\_Coronal} \\ \mu \text{ LPLGF\_Coronal} \\ \mu \text{ LMGF\_Coronal} \end{array} \right\} \neq \left\{ \begin{array}{l} 0 \\ 0 \\ 0 \\ 0 \\ 0 \\ 0 \end{array} \right\}$$



$$\text{Ha2.1} \left[ \begin{array}{c} \mu \text{ RLC\_Axial} \\ \mu \text{ RMC\_Axial} \\ \mu \text{ RPC\_Axial} \\ \mu \text{ RALGF\_Axial} \\ \mu \text{ RPLGF\_Axial} \\ \mu \text{ RMGF\_Axial} \\ \mu \text{ LLC\_Axial} \\ \mu \text{ LMC\_Axial} \\ \mu \text{ LPC\_Axial} \\ \mu \text{ LALGF\_Axial} \\ \mu \text{ LPLGF\_Axial} \\ \mu \text{ LMGF\_Axial} \end{array} \right] \neq \left[ \begin{array}{c} 0 \\ 0 \\ 0 \\ 0 \\ 0 \\ 0 \\ 0 \\ 0 \\ 0 \\ 0 \\ 0 \\ 0 \end{array} \right]$$

- Concerning the condyle:

$$\text{H02.2} \left\{ \begin{array}{l} \mu \text{ RLC\_Axial} \\ \mu \text{ RMC\_Axial} \\ \mu \text{ RPC\_Axial} \\ \mu \text{ LLC\_Axial} \\ \mu \text{ LMC\_Axial} \\ \mu \text{ LPC\_Axial} \end{array} \right\} = \left\{ \begin{array}{l} 0 \\ 0 \\ 0 \\ 0 \\ 0 \\ 0 \end{array} \right\}$$

$$\text{Ha2.2} \left\{ \begin{array}{l} \mu \text{ RLC\_Axial} \\ \mu \text{ RMC\_Axial} \\ \mu \text{ RPC\_Axial} \\ \mu \text{ LLC\_Axial} \\ \mu \text{ LMC\_Axial} \\ \mu \text{ LPC\_Axial} \end{array} \right\} \neq \left\{ \begin{array}{l} 0 \\ 0 \\ 0 \\ 0 \\ 0 \\ 0 \end{array} \right\}$$

- Concerning the glenoid fossa:

$$\begin{array}{l}
 \text{H02.3} \\
 \left. \begin{array}{l}
 \mu \text{ RALGF\_Axial} \\
 \mu \text{ RPLGF\_Axial} \\
 \mu \text{ RMGF\_Axial} \\
 \mu \text{ LALGF\_Axial} \\
 \mu \text{ LPLGF\_Axial} \\
 \mu \text{ LMGF\_Axial}
 \end{array} \right\} = \left. \begin{array}{l}
 0 \\
 0 \\
 0 \\
 0 \\
 0 \\
 0
 \end{array} \right\}
 \end{array}$$

$$\begin{array}{l}
 \text{Ha2.3} \\
 \left. \begin{array}{l}
 \mu \text{ RALGF\_Axial} \\
 \mu \text{ RPLGF\_Axial} \\
 \mu \text{ RMGF\_Axial} \\
 \mu \text{ LALGF\_Axial} \\
 \mu \text{ LPLGF\_Axial} \\
 \mu \text{ LMGF\_Axial}
 \end{array} \right\} \neq \left. \begin{array}{l}
 0 \\
 0 \\
 0 \\
 0 \\
 0 \\
 0
 \end{array} \right\}
 \end{array}$$

3- Concerning the mediolateral positional change:

- Condyle and glenoid fossa

$$\begin{matrix} & \left[ \begin{array}{c} \mu \text{ RLC\_Sagittal} \\ \mu \text{ RMC\_Sagittal} \\ \mu \text{ RPC\_Sagittal} \\ \mu \text{ RALGF\_Sagittal} \\ \mu \text{ RPLGF\_Sagittal} \\ \mu \text{ RMGF\_Sagittal} \\ \mu \text{ LLC\_Sagittal} \\ \mu \text{ LMC\_Sagittal} \\ \mu \text{ LPC\_Sagittal} \\ \mu \text{ LALGF\_Sagittal} \\ \mu \text{ LPLGF\_Sagittal} \\ \mu \text{ LMGF\_Sagittal} \end{array} \right] & = & \left[ \begin{array}{c} 0 \\ 0 \\ 0 \\ 0 \\ 0 \\ 0 \\ 0 \\ 0 \\ 0 \\ 0 \\ 0 \\ 0 \end{array} \right] \end{matrix}$$

H03.1

Ha3.1	$\mu$ RLC_Sagittal	$\neq$	0
	$\mu$ RMC_Sagittal		0
	$\mu$ RPC_Sagittal		0
	$\mu$ RALGF_Sagittal		0
	$\mu$ RPLGF_Sagittal		0
	$\mu$ RMGF_Sagittal		0
	$\mu$ LLC_Sagittal		0
	$\mu$ LMC_Sagittal		0
	$\mu$ LPC_Sagittal		0
	$\mu$ LALGF_Sagittal		0
	$\mu$ LPLGF_Sagittal		0
	$\mu$ LMGF_Sagittal		0

- Concerning the condyle:

$$\text{H03.2} \left\{ \begin{array}{l} \mu \text{ RLC\_Sagittal} \\ \mu \text{ RMC\_Sagittal} \\ \mu \text{ RPC\_Sagittal} \\ \mu \text{ LLC\_Sagittal} \\ \mu \text{ LMC\_Sagittal} \\ \mu \text{ LPC\_Sagittal} \end{array} \right\} = \left\{ \begin{array}{l} 0 \\ 0 \\ 0 \\ 0 \\ 0 \\ 0 \end{array} \right\}$$

$$\text{Ha3.2} \left\{ \begin{array}{l} \mu \text{ RLC\_Sagittal} \\ \mu \text{ RMC\_Sagittal} \\ \mu \text{ RPC\_Sagittal} \\ \mu \text{ LLC\_Sagittal} \\ \mu \text{ LMC\_Sagittal} \\ \mu \text{ LPC\_Sagittal} \end{array} \right\} \neq \left\{ \begin{array}{l} 0 \\ 0 \\ 0 \\ 0 \\ 0 \\ 0 \end{array} \right\}$$

- Concerning the glenoid fossa:

$$\text{H03.3} \left\{ \begin{array}{l} \mu \text{ RALGF\_Sagittal} \\ \mu \text{ RPLGF\_Sagittal} \\ \mu \text{ RMGF\_Sagittal} \\ \mu \text{ LALGF\_Sagittal} \\ \mu \text{ LPLGF\_Sagittal} \\ \mu \text{ LMGF\_Sagittal} \end{array} \right\} = \left\{ \begin{array}{l} 0 \\ 0 \\ 0 \\ 0 \\ 0 \\ 0 \end{array} \right\}$$

$$\text{Ha3.3} \left\{ \begin{array}{l} \mu \text{ RALGF\_Sagittal} \\ \mu \text{ RPLGF\_Sagittal} \\ \mu \text{ RMGF\_Sagittal} \\ \mu \text{ LALGF\_Sagittal} \\ \mu \text{ LPLGF\_Sagittal} \\ \mu \text{ LMGF\_Sagittal} \end{array} \right\} \neq \left\{ \begin{array}{l} 0 \\ 0 \\ 0 \\ 0 \\ 0 \\ 0 \end{array} \right\}$$